Designation: E3057 – 19

Standard Test Method for Measuring Heat Flux Using Directional Flame Thermometers with Advanced Data Analysis Techniques[1]

This standard is issued under the fixed designation E3057; the number immediately following the designation indicates the year of original adoption or, in the case of revision, the year of last revision. A number in parentheses indicates the year of last reapproval. A superscript epsilon (ε) indicates an editorial change since the last revision or reapproval.

INTRODUCTION

This test method describes a technique for measuring the net heat flux to one or both surfaces of a sensor called a Directional Flame Thermometer. The sensor covered by this standard uses measurements of the temperature response of two metal plates along with a thermal model of the sensor to determine the net heat flux. These measurements can be used to estimate the total heat flux (also known as thermal exposure) and bi-directional heat fluxes for use in CFD thermal models.

The development of Directional Flame Thermometers (DFTs) as a device for measuring heat flux originated because commercially available, water-cooled heat flux gauges (for example, Gardon and Schmidt-Boelter gauges) did not work as desired in large fire tests. Because the Gardon and Schmidt-Boelter (S-B) gauges are water cooled, condensation and soot deposition can occur during fire testing or in furnaces. Both foul the sensing surface which in turn changes the sensitivity (calibration) of the gauge. This results in an error during data reduction. Therefore, a different type of sensor was needed; one such sensor is a DFT. DFTs are not cooled so condensation and soot deposition are minimized or eliminated.

Additionally, a body of work has shown that for both Gardon and Schmidt-Boelter gauges the sensitivity coefficients determined through the calibration process, which uses a radiative heat source, are not the same as the sensitivity coefficients determined if a purely convective source is used for calibration [Test Method E511-07; Keltner and Wildin, 1975 (**1, 2**); Borell, G. J., and Diller, T. E., 1987 (**3**); Gifford, A., et al., 2010 (**4**); Gritzo, L. A., et al., 1995 (**5**); Young, M. F., 1984 (**6**); Sobolik, et al., 1987 (**7**); Kuo and Kulkarni, 1991 (**8**); Keltner, 1995 (**9**); Gifford, et al., 2010 (**10**); Nakos, J. T., and Brown, A. L., 2011 (**11**)].[2] As a result, one can incur significant bias errors when reducing data in tests where there may be a non-negligible convective component because the only sensitivity coefficient available is for a radiation calibration. It was desired to reduce/eliminate these potential sources of error by designing a gauge that does not depend on a radiation only calibration. DFTs have this characteristic.

A sensor, also called a Directional Flame Thermometer, was developed to help estimate flame thickness in pool fire tests of hazardous material shipping containers [Burgess, M. H., 1986 (**12**); Fry, C. J., 1989 (**13**); Burgess, M. H., et al., 1990 (**14**); and Fry, C. J., 1992 (**15**)]. As originally designed, DFTs were quasi-equilibrium sensors that used a thin metal plate with a single thermocouple attached and backed by multiple radiation shields. To make a sensor suitable for continuous transient heat flux measurements, this basic design was modified to use two instrumented plates, with a layer of insulation in between.

For the Directional Flame Thermometers described in this standard, the net heat flux is calculated using transient temperature measurements of the two plates and temperature dependent material properties for the plates and the insulation. Three methods are described in this standard to calculate the net heat flux. The most accurate method for calculating the net heat flux is believed to be the 1-dimensional, nonlinear inverse heat conduction analysis, which uses the IHCP1D code. This is based on uncertainty analyses and comparisons with measurements made with Schmidt-Boelter and Gardon gauges, which have NIST traceable calibrations. The second method uses transient energy balances on the DFT. As will be shown below, the energy balance method compares very well with the inverse method, again based on uncertainty analyses. The third method uses sets of linearized, convolution digital filters based on IHCP1D. These allow a near real-time calculation of the net heat flux [Keltner, N. R., 2007 (**16**); Keltner, N. R., et al., 2010 (**17**)]. See Section 1 for more detailed information on each

analysis technique. Additional information is given in the Annexes and Appendices.

Various DFT designs have been used in a variety of applications including very large pool fires, LNG spill fires, marine fire safety testing, automobile fires, to study rocket launch accident fires, and in research of forest and wild-land fires. Appendix X1 provides a comprehensive list of applications where DFTs have been successfully used.

Advantages of DFTs are their relatively low cost, ease of construction, they require no calibration (see later), and require no cooling. They are robust and can survive intense fire environments without failure. Disadvantages include most are large compared with Gardon and S-B heat flux gauges and because they are not calibrated, one cannot reference the measurements to a NIST standard. Because no calibration is required, one must quantify the uncertainties present in the temperature measurements and the data reduction methods used to calculate the heat flux. Also, DFTs measure net heat flux; for a direct comparison with Gardon and S-B gauges, which are calibrated to incident (or "cold wall") flux, one must use a thermal model to estimate the incident flux.

The best applications for DFTs are where Gardon and S-B gauges cannot be used (for example, due to high temperatures, lack of cooling, soot deposition, fouling, and so forth), or when long life and overall costs are a consideration. Gardon and Schmidt-Boelter gauges are recommended in non-sooty environments, when it is possible to mount the gauges and cooling lines, and in predominantly radiative environments with a small convective contribution.

---

[1] This test method was jointly developed by ASTM Committee E21 on Space Simulation and Applications of Space Technology and is the direct responsibility of Subcommittee E21.08 on Thermal Protection.

Current edition approved June 1, 2019. Published July 2019. Originally approved in 2016. Last previous edition approved in 2016 as E3057 – 16. DOI: 10.1520/E3057-19.

[2] The boldface numbers in parentheses refer to the list of references at the end of this standard.

1. Scope

1.1 This test method describes the continuous measurement of the hemispherical heat flux to one or both surfaces of an uncooled sensor called a "Directional Flame Thermometer" (DFT).

1.2 DFTs consist of two heavily oxidized, Inconel 600 plates with mineral insulated, metal-sheathed (MIMS) thermocouples (TCs, type K) attached to the unexposed faces and a layer of ceramic fiber insulation placed between the plates.

1.3 Post-test calculations of the net heat flux can be made using several methods. The most accurate method uses an inverse heat conduction code. Nonlinear inverse heat conduction analysis uses a thermal model of the DFT with temperature dependent thermal properties along with the two plate temperature measurement histories. The code provides transient heat flux on both exposed faces, temperature histories within the DFT as well as statistical information on the quality of the analysis.

1.4 A second method uses a transient energy balance on the DFT sensing surface and insulation, which uses the same temperature measurements as in the inverse calculations to estimate the net heat flux.

1.5 A third method uses Inverse Filter Functions (IFFs) to provide a near real time estimate of the net flux. The heat flux history for the "front face" (either surface exposed to the heat source) of a DFT can be calculated in real-time using a convolution type of digital filter algorithm.

1.6 Although developed for use in fires and fire safety testing, this measurement method is quite broad in potential fields of application because of the size of the DFTs and their construction. It has been used to measure heat flux levels above 300 kW/m^2 in high temperature environments, up to about 1250 °C, which is the generally accepted upper limit of Type K or N thermocouples.

1.7 The transient response of the DFTs is limited by the response of the MIMS TCs. The larger the thermocouple the slower the transient response. Response times of approximately 1 to 2 s are typical for 1.6 mm diameter MIMS TCs attached to 1.6 mm thick plates. The response time can be improved by using a differential compensator.

1.8 The values stated in SI units are to be regarded as standard. The values given in parentheses after SI units are provided for information only and are not considered standard.

1.9 *This standard does not purport to address all of the safety concerns, if any, associated with its use. It is the responsibility of the user of this standard to establish appropriate safety, health, and environmental practices and determine the applicability of regulatory limitations prior to use.*

1.10 *This international standard was developed in accordance with internationally recognized principles on standardization established in the Decision on Principles for the Development of International Standards, Guides and Recommendations issued by the World Trade Organization Technical Barriers to Trade (TBT) Committee.*

2. Referenced Documents

2.1 *ASTM Standards:*[3]

C177 Test Method for Steady-State Heat Flux Measurements and Thermal Transmission Properties by Means of

---

[3] For referenced ASTM standards, visit the ASTM website, www.astm.org, or contact ASTM Customer Service at service@astm.org. For *Annual Book of ASTM Standards* volume information, refer to the standard's Document Summary page on the ASTM website.

the Guarded-Hot-Plate Apparatus
E119 Test Methods for Fire Tests of Building Construction and Materials
E176 Terminology of Fire Standards
E457 Test Method for Measuring Heat-Transfer Rate Using a Thermal Capacitance (Slug) Calorimeter
E459 Test Method for Measuring Heat Transfer Rate Using a Thin-Skin Calorimeter
E511 Test Method for Measuring Heat Flux Using a Copper-Constantan Circular Foil, Heat-Flux Transducer
E1529 Test Methods for Determining Effects of Large Hydrocarbon Pool Fires on Structural Members and Assemblies
E2683 Test Method for Measuring Heat Flux Using Flush-Mounted Insert Temperature-Gradient Gages

2.2 *Other Standards:*

ISO 834-11:2014 Fire Resistance Tests—Elements of Building Construction—Part 11: Specific Requirements for the Assessment of Fire Protection to Structural Steel Elements[4]
IMO A754 Fire Resistance Tests: Fire Safety Onboard Ships[5]

2.3 *Other ASTM Document:*[6]

MNL12-4th Manual on the Use of Thermocouples in Temperature Measurement, Fourth Edition, 1993, Sponsored by ASTM Committee E20 on Temperature Measurement

3. Terminology

3.1 *Definitions*—Refer to Terminology E176 for definitions of some terms used in these test methods.

3.2 *Definitions of Terms Specific to This Standard:*

3.2.1 *incident radiative heat flux (irradiance; $q_{inc,r}$), n*—radiative heat flux impinging on the surface of the DFT or the unit under test.

3.2.2 *net heat flux, n*—storage in the DFT front plate + transmission (in other words, loss) to insulation layer. It is equal to the [absorbed radiative heat flux + convective heat flux] – [re-radiation from the exposed surface].

3.2.3 *total absorbed heat flux, n*—absorbed radiative heat flux + convective flux.

3.2.4 *total cold wall heat flux, n*—the heat flux that would be transferred by means of convection and radiation to an object whose temperature is 21 °C (70 °F).

3.2.5 *total heat flux (thermal exposure), n*—incident radiative heat flux + convective heat flux.

4. Summary of Test Method

4.1 This test method provides techniques for measurement of the net heat flux to a surface. Because Directional Flame Thermometers are un-cooled devices, they are minimally affected by soot deposition or condensation. Calibration factors or sensitivity coefficients are not required because alternate methods of data reduction are used. DFTs are simple to fabricate and use, but are more complicated when reducing the data. Gardon and Schmidt-Boelter gauges have relatively linear outputs with heat flux and only require a single sensitivity coefficient (for example, xx mv/unit of flux) to convert the output to an incident heat flux. DFTs have two thermocouple outputs as a function of time. Those outputs along with temperature dependent thermal properties and advanced analysis techniques are used with a thermal model to calculate the net heat flux. The net heat flux (with an energy balance) can be used to estimate the total cold wall heat flux, which is same as the measurement made by Gardon or S-B gauges [Janssens, 2007 (**18**)].

5. Significance and Use

5.1 *Need for Heat Flux Measurements:*

5.1.1 Independent measurements of temperature and heat flux support the development and validation of engineering models of fires and other high environments, such as furnaces. For tests of fire protection materials and structural assemblies, temperature and heat flux are necessary to fully specify the boundary conditions, also known as the thermal exposure. Temperature measurements alone cannot provide a complete set of boundary conditions.

5.1.2 Temperature is a scalar variable and a *primary variable*. Heat Flux is a vector quantity, and it is a *derived variable*. As a result, they should be measured separately just as current and voltage are in electrical systems. For steady-state or quasi-steady state conditions, analysis basically uses a thermal analog of Ohm's Law. The thermal circuit uses the temperature difference instead of voltage drop, the heat flux in place of the current and thermal resistance in place of electrical resistance. As with electrical systems, the thermal performance is not fully specified without knowing at least two of these three parameters (temperature drop, heat flux, or thermal resistance). For dynamic thermal experiments like fires or fire safety tests, the electrical capacitance is replaced by the volumetric heat capacity.

5.1.3 The net heat flux, which is measured by a DFT, is likely different than the heat flux into the test item of interest because of different surface temperatures. An alternative measurement is the total cold wall heat flux which is measured by water-cooled Gardon or S-B gauges. The incident radiative flux can be estimated from either measurement by use of an energy balance [Keltner, 2007 and 2008 (**16, 17**)]. The convective flux can be estimated from gas temperatures and the convective heat transfer coefficient, h [Janssens, 2007 (**18**)]. Assuming the sensor is physically close to the test item of interest; one can use the incident radiative and convective fluxes from the sensor as boundary conditions into the test item of interest.

5.1.4 In standardized fire resistance tests such as Test Methods E119 and E1529, or ISO 834 or IMO A754, the furnace temperature is controlled to a standard time-temperature curve. In all but Test Methods E1529, implicit assumptions have been made that the thermal exposure can be described solely by the measured furnace temperature history and that it will be repeatable from time to time and place to

[4] Available from American National Standards Institute (ANSI), 25 W. 43rd St., 4th Floor, New York, NY 10036, http://www.ansi.org.
[5] Available from International Maritime Organization (IMO), 4, Albert Embankment, London SE1 7SR, United Kingdom, http://www.imo.org.
[6] Available from the ASTM website, www.astm.org, or contact ASTM Customer Service at service@astm.org.

place. However, these tests provide very different thermal exposures due to the use of temperature sensors with very different designs for furnace control. As a result, these different thermal exposure histories produce different fire ratings for the same item. Historical variations of up to 50 % or more in the qualitative fire protection ratings (for example, 1 h) between different furnaces or laboratories indicate that the assumptions for time-temperature control are not well founded. Also, due to different sensors, thermal exposure in a vertical furnace is generally higher than in a horizontal furnace, and thermal exposure on the floor of a horizontal furnace is generally higher than on the ceiling. These reasons provide support for why both temperature and heat flux measurements are needed to provide consistent test results.

5.1.5 In the mid-90's, the U. S. Coast Guard authorized a study of the problems in marine fire resistance tests, such as large variations in the ratings obtained in different furnaces. One important conclusion was that the thermal exposure in furnaces could not be predicted solely from furnace temperature measurements without large static and dynamic uncertainties [Wittasek, N. A., 1996 (**19**)].

5.1.6 One of the recommendations that resulted from NIST's investigation of the World Trade Center disaster was the need to move towards performance based codes and standards. A report developed for The Fire Protection Research Foundation expanded on this recommendation [Beyler, C., et al., 2008 (**20**)]. Part of this effort involves making a more comprehensive set of measurements in fire resistance tests including quantitative heat flux measurements. It also involves the development and use of "design fires" and defining their relationship with standardized test methods.

5.1.7 Work at Sandia National Laboratories on transportation accidents involving hazardous materials compares the Prescriptive and Performance based approaches [Tieszen, et al., 2010 (**21**)].

5.1.8 Work by the National Research Council of Canada used four (4) different temperature sensors to control a horizontal furnace. Differences in the thermal exposure (see definition in 3.2.5) were as high as 100 % during the first 10 min [Sultan, M., 2006 and 2008 (**22, 23**)]. Assuming the temperature measurements from the different sensors or different installations of the same sensor are actually the furnace temperature, one can predict very different thermal exposures depending on which temperature measurement method is used.

5.1.9 In another series of horizontal furnace tests, the National Research Council of Canada (NRCC) studied the effect of six (6) different temperature sensor designs on fire resistance tests in a large, horizontal furnace [Sultan, 2008 (**23**)]. NRCC used six different temperature sensors for furnace control: Test Methods E119 Shielded Thermocouple, ISO 834 Plate Thermometer, 6 mm MIMS TC from Test Methods E1529, Directional Flame Thermometers, and 1.6 mm MIMS TCs with grounded and ungrounded junctions. Total heat flux at the ceiling was measured using a Gardon gauge. Results showed that very different thermal exposures are possible depending on the measurement method used. During the first 10 min of a fire resistance test, the integrated heat flux varies by a factor of two.

5.1.10 Reports by Sultan, M., (2006 and 2008) (**22, 23**) and Janssens, M., (2008) (**18**) have shown it is difficult to measure one parameter in a fire resistance test (such as the furnace temperature) and calculate the other (heat flux or thermal exposure).

5.1.11 From the discussions in 5.1, it is highly recommended that both temperature and heat flux be measured independently in fire tests.

5.2 *Use for DFTs:*

5.2.1 Although both cooled and non-cooled sensors can be used to measure heat flux, the results are generally quite different. Water-cooled sensors are the direct reading Schmidt-Boelter or Gardon gauge designs that are used in some Committee E5 Methods (Test Methods E2683 and E511, respectively, have been developed for these sensors by Subcommittee E21.08).

5.2.2 There are three types of passive or un-cooled sensors that can be used to measure net heat flux. One is the hybrid sensor (so-called High Temperature Heat Flux Sensor, HTHFS) developed by Diller, et al., at Virginia Tech. It is designed to measure heat transfer to a surface without water cooling [Gifford, A., Hubble, D., Pullins, C., and Diller, T., 2010 (**4**)]. The HTHFS requires a calibration factor that is a function of sensor temperature [Pullins and Diller, 2010 (**24**)]. Another is the so-called "direct write heat flux sensor" which can be used at temperatures from 25 to 860 °C [Trelewicz, Longtin, Hubble, and Greenlaw, 2015 (**25**)]; this gauge requires a calibration coefficient. The third is the Directional Flame Thermometer (DFT), which was developed at Sandia National Laboratories (based on work in the UK) and elsewhere for measuring heat transfer in large sooty pool fires. DFTs do not require a calibration factor, which may be viewed as a mixed benefit. The passive sensors typically have higher temperature capability, based mainly on the Type K or N TC limit of about 1250 °C. Even though they are water cooled, quite often Gardon and Schmidt-Boelter gauges do not survive in temperatures due to fouling of the sensing surface, and other effects. DFTs usually survive up to about 1100 °C. They are very rugged, require no cooling, and are not susceptible to fouling of the sensing surface. These characteristics simplify installation in a wide range of fire and other applications. This standard will only address DFTs. See 10.2.2 for a more thorough discussion of heat flux gauge calibrations.

5.2.3 Early work on DFTs (and the data analysis techniques for them) focused on acquiring quantitative heat flux data to help define the thermal conditions in large, liquid hydrocarbon pool or spill fires. Large pool fires can reach quasi-steady conditions in times as short as a minute. As a result, Pool Fire DFTs were designed with 1.6 mm thick plates to provide rapid equilibration with the fire (the maximum heating rate in these fires was approximately 30 °C/s).

6. Apparatus

6.1 *DFT Construction:*

6.1.1 DFT apparatus consists of the DFT, mounting hardware, and a data acquisition system.

6.1.2 The DFT consists of two heavily oxidized Inconel plates with a ceramic fiber insulation layer sandwiched between the plates. Alternately, to obtain a high emissivity surface one can apply high emissivity paint to the exposed surface. If paint is used, one must be careful as at high temperatures some paints do not remain in place. A 1.6 mm OD, mineral-insulated, metal-sheathed (MIMS) thermocouple (TC) is attached to each unexposed face. Typically the sheath material is Inconel. To optimize the response in a variety of fire scenarios, there are three basic DFT designs. The original furnace DFT uses two 3 mm (nominal) thick plates; the original pool fire DFT uses two 1.6 mm (nominal) thick plates. Both Inconel and SS have been used; Inconel 600 is recommended because 304SS can sometimes form a scale that falls off the surface. The modified furnace DFT uses a 3 mm plate facing into the furnace with a 1.6 mm back plate. Different plate thicknesses are used for different applications. Some special designs have used a third plate and thermocouple. Some used in automotive fires were small and used intrinsic thermocouples[7] to provide very fast response. Fig. 1 shows the construction of a typical DFT, and Fig. 2 shows a photo of a typical DFT.

6.1.3 Plate thicknesses vary depending on the application. If faster response is desired a thinner plate is used (for example, 1.6 mm), or if slower response is acceptable, a thicker plate can be used (for example, 3 mm). It is advisable to never have the plate thickness less than the TC sheath diameter, so the effect of the TC on the plate temperature measurement is minimized [see Figueroa, 2005 (**26-28**) for a detailed analysis]. Due to

[7] Intrinsic thermocouples use bare wires welded to the metal surface of the DFT. This forms an "intrinsic" junction using the metal of the DFT. Intrinsic TCs have small dynamic errors compared with ungrounded junction (sheathed) TCs but are not very robust and fail more often. MIMS TCs are fully sheathed and encase the TC junction, and can be grounded or ungrounded.

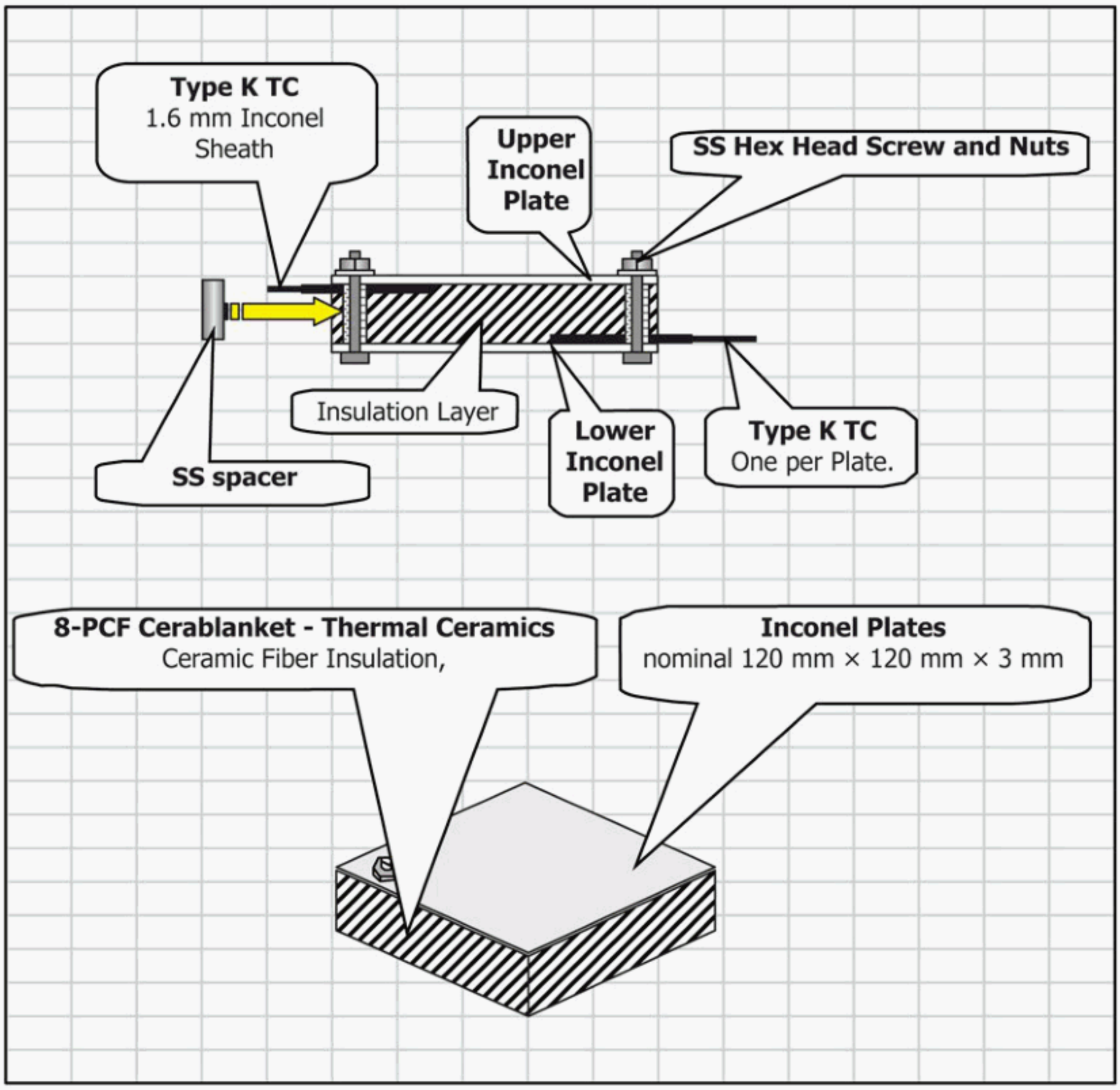

FIG. 1 Basic Design of a Directional Flame Thermometer (Using 3 mm Thick Plates)

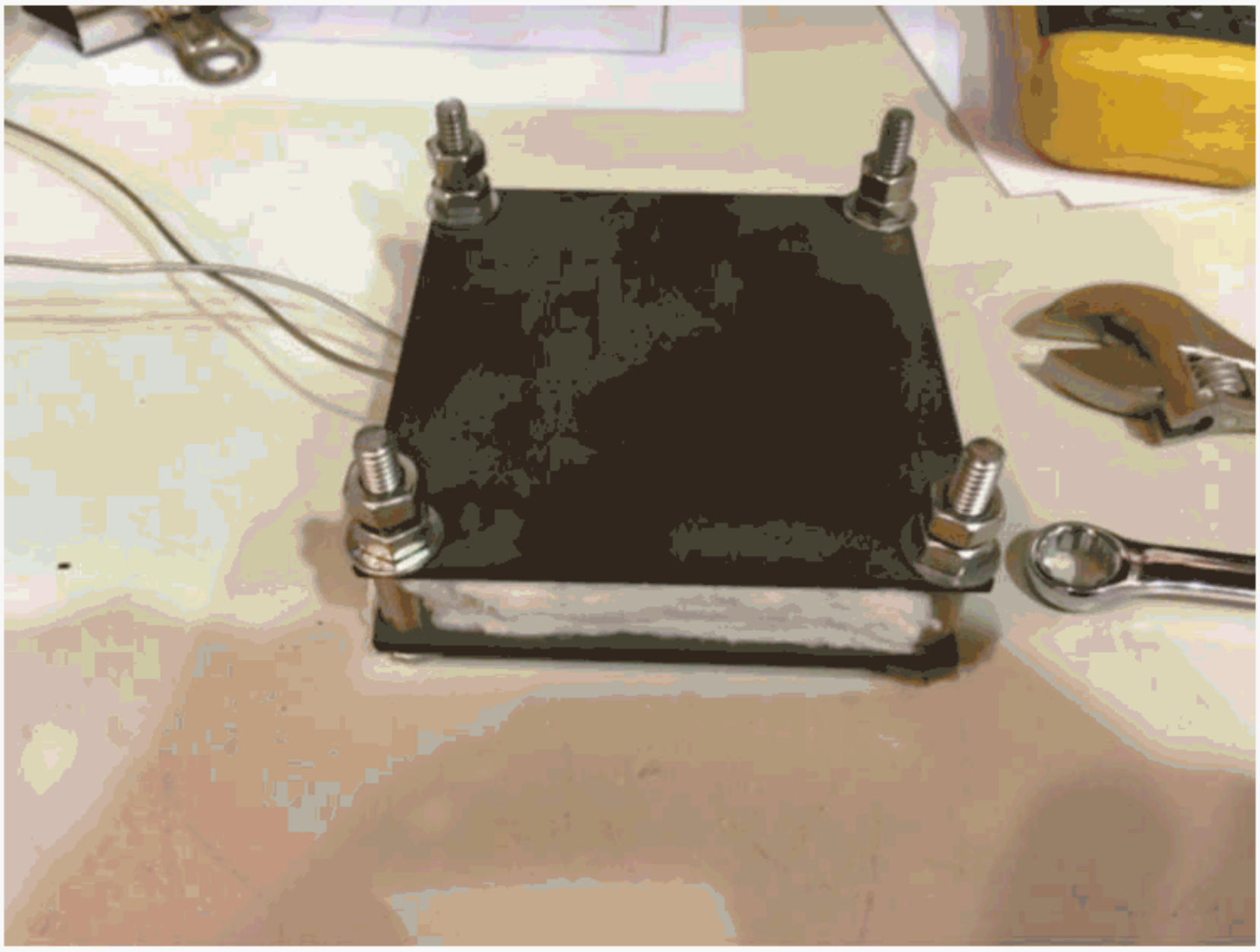

FIG. 2 Photo of Typical DFT

manufacturers recommended limits on MIMS thermocouples, TC sheath diameters less than 1.6 mm are not recommended.

6.1.4 The Inconel plates are mounted parallel with a layer of ceramic fiber insulation material lightly compressed in between the plates. The plates are held together with four bolts. One thermocouple is mounted on the inside surface of each of the Inconel plates. A 12 mm wide by 25 mm long strip of nickel or Nichrome foil (for example, 0.08 mm thick) is formed over the tip of the thermocouple and spot welded to the unexposed surface of each plate (see Fig. 3). This technique provides a good thermo-mechanical attachment of the thermocouples, which is critical for good dynamic response In general the

FIG. 3 Photo of Typical TC Installation

nichrome strip should be as small as possible while still ensuring good mechanical contact with the surface (see MNL12, page 183). Fig. 3 shows a typical TC installation.

6.1.5 Apparatus to mount the DFT near the test unit should be as small as possible to disturb the environment as little as possible. The DFT should be mounted so that one of the Inconel plates is facing the environment one wants to measure. The DFT has a 180° field of view, so the DFT should be oriented so that the entire environment is captured within that field of view.

6.1.6 The data acquisition system needs to be able to accurately record Type K or Type N thermocouples. Many such systems exist and we will not discuss them further here.

7. Preparation of Apparatus

7.1 *Fabrication of Directional Flame Thermometers:*

7.1.1 See Fig. 1 for a sketch of a DFT.

7.1.2 See Fig. 2 for a photograph of a DFT.

7.1.3 Cut or shear two 1.6 or 3 mm (1⁄16 or 0.12 in.) thick Inconel plates, 120 mm^2 (4.75 $in.^2$).

7.1.4 Drill 6.75 mm (letter drill H, 17⁄64 in.) holes in four corners, leaving approximately one hole diameter from each edge.

7.1.5 Heat the plates in a furnace at approximately 1000 °C for 24 h to develop a stable, high absorptivity oxide layer.[8] If this is not possible, one can substitute a high emissivity paint that adheres to the plate at high temperatures.

7.1.6 Use 1.6 mm (1⁄16 in.) OD Inconel sheathed Type K (Chromel/Alumel) or Type N thermocouples (TCs) with an ungrounded junction. Sand the oxide off the plate over a 3 by 1.5–3.9 cm (1.2 by 0.6–1.3 in.) area in the center of each plate.

7.1.7 Using 0.08 mm (0.003 in.) thick by 6.4 mm (0.25 in.) wide Nickel or Nichrome foil, form the foil strips tightly over last 25 mm (1 in.) of the TC and completely cover the TC tip. Then, spot weld the foil to the sanded area of the plate (do not spot weld to the TC sheath). Provide a loop for stress relief. Do not weld the TC because the welding process might penetrate through the sheath. See Fig. 3 (in the photo the strap is shorter than recommended).

7.1.8 Cut a 120 by 120 by 25 mm (4.75 by 4.75 by 1 in.) piece of 128 kg/m^3 (8 lb/ft^3) ceramic fiber insulation and place between the plates. Temperature dependent thermal properties of a Thermal Ceramics insulation called "Cerablanket" have been measured, and those properties are provided in Annex A1. If a different insulation is used, it is important to measure the properties of that material. There are other brands (for example, Kaowool by Morgan Thermal Ceramics, http://www.morganthermalceramics.com/products/refractory-ceramic-fibre-rcf/blanket) that can be used, but the temperature dependent, thermal properties would need to be measured.

7.1.9 Assemble the DFT using four 9.53 mm (~3⁄8 in. diameter) Inconel 600 or silver plated SS bolts and tubular spacers (for example, made of 304 stainless steel) to compress the insulation layer to a thickness of 19 mm (0.75 in.). This compression is important because the insulation thermal properties depend on thickness. See Annex A1.

7.1.10 Route the two TCs together out of the heated region. It is recommended that the TC sheaths be insulated until they reach a room temperature location.

7.2 *Fabrication of Mounting Hardware*—Mounting hardware is not unique. Any mounting design that holds the DFT in place but does not affect the environment is suitable. Any material that can withstand the temperatures in the environment of interest can be used. Mild steel can be used if the melt temperature is not exceeded. But recall that the strength of mild steel at high temperatures is reduced to approximately that of aluminum, so strength is much reduced. Stainless steel is the better, but more expensive option.

8. Hazards

8.1 This standard does not purport to address all of the safety concerns, if any, associated with the use of DFTs. It is the responsibility of the user of this standard to establish appropriate safety and health practices and determine the applicability of regulatory limitations prior to use.

8.2 **Warning—**The only known potential hazard is related to the insulation in the DFT. Long durations in unventilated areas with used insulation may be cause for concern because some of the ceramic fibers may become airborne. The user should contact the insulation manufacturer for information about proper safety procedures related to the insulation.

9. Procedure

9.1 Fabricate DFT in accordance with 7.1 and the mounting hardware in accordance with 7.2.

9.2 Mount the DFT so that the field of view of the DFT encompasses the entire heat source.

9.3 Route the two thermocouple leads to a room temperature location. The TC sheaths should be protected from the heat source by wrapping them with the same type of insulation used in the DFT. This protection can reduce the chance of "shunting" occurring. See Appendix X3.2.

9.4 Calibrate the DAS by using a NIST traceable source to place a known input into each channel at a select number of temperatures to ensure each DAS channel is reading properly.

9.5 Connect the TCs to a data acquisition system (DAS).

9.6 Do not calibrate the TCs used in the DFT, because for Type K TCs the calibration process can change the output of the TC and therefore change the calibration (**30**, **31**).

9.7 Set up DAS to scan at a rate of about 1 Hz. Because the time constant of the TCs can be several seconds, there is no reason to sample at a faster rate.

9.8 Measure pre- and post-test emissivity of the exposed DFT plate surfaces. These measurements can be used to estimate the incident heat flux.

[8] Work at Sandia National Laboratories has shown the Inconel emissivity can vary considerably depending on the extent of the oxide layer. Values of about 0.85 have been measured [for example, Figueroa, 2006 (**26-28**)], but others [Brundage, A., et al (**29**)] measured emissivity between 0.67 and 0.90. For highest accuracy the user should either measure the emissivity measurements or apply high emissivity black paint with known emissivity.

9.9 Carefully review thermocouple results to ensure anomalies are not present (for example, a spike in temperature that has no basis for occurring).

9.10 Reduce data by means of one of the methods described below.

10. Calibration and Standardization

10.1 *Apparatus Calibration*—Two items should be calibrated when using DFTs, the data acquisition system and the thermocouples. However, the thermocouples should be "calibrated" in a manner different than is typically done.

10.1.1 *Thermocouple "Calibration"*—The ASTM standards for accuracy are sufficiently good for use in DFTs. It has been shown that Type K thermocouples are actually affected by the calibration process. As a result, the chemistry of the Chromel and Alumel wires change when calibrated above about 320 °C (**30, 31**). TCs used in DFTs should be calibrated up to the maximum temperature expected (for example, 1100 °C). Therefore, one should not use the TC after calibration. This apparent conundrum is resolved in the following manner. One can obtain additional TCs fabricated from the same spool of wire from the manufacturer (preferably wire before and after the TCs used on the DFTs). Those additional TCs are sent through the calibration process. If those calibrated TCs meet or exceed the ASTM standard for Type K TCs (in other words, ±2.2 °C or ±0.75 % of reading in °C, see MNL12, 1993), then one assumes the remaining TCs from the same spool also meet the same ASTM standard. Experience has shown that in all cases the calibrated TCs were more accurate than the ASTM standard. But the more accurate values are not used; one uses the accuracy specifications from the MNL12, so as not to assume accuracy better than the standard.

10.1.2 *Data Acquisition System Calibration*—The recommended method to assure that the data acquisition system uncertainty is known is to calibrate each channel over the range of temperatures expected. For example, if one expects temperatures ranging from 20 to 1100 °C, one can calibrate at several set points over the range (for example, 20, 200, 400, 600, 800, 1100 °C). The calibration is performed using a NIST traceable thermocouple simulator (for example, Fluke and Ectron make such calibrators). A statistically significant sample (for example, 10s of samples) is taken at each set point, then the mean and standard deviation of each set point on each channel can be estimated. Because this can be a very large data set, one can average the data for all channels at all set points to provide a single estimate of the accuracy of all DAS channels. Typically this source of uncertainty is small, but on occasion one finds a bad channel so the exercise is worthwhile.

10.1.3 *Detailed Measurements of DFT*—Detailed measurements of the DFT materials should be made before assembly, because those measurements will be used in the data reduction process.

10.1.3.1 Measure and record the thickness of both Inconel plates as close to the center as possible. Estimate the accuracy of those measurements.

10.1.3.2 Measure and record the spacer thicknesses to confirm they are 1.91 cm (0.75 in.).

10.1.3.3 Verify insulation (8 lb/ft^3) is compressed to 1.91 cm thickness and is not forced out the sides of the plates. If the insulation is different from Cerablanket, measure the temperature dependent thermal properties. See Annex A1.

10.1.3.4 Verify the TCs are mounted according to the procedure in 7.1.

10.1.3.5 Verify the plate surfaces have a stable oxidation layer or stable paint layer (if one cannot oxidize the plates at 1000 °C, an alternate is to use a high absorptivity paint).

10.1.3.6 Measure and record the hemispherical total surface emissivity of exposed surfaces of each plate. This is used if one desires to convert the net heat flux to incident heat flux. Estimate the emissivity uncertainty by making multiple measurements and using the manufacturer's reported accuracy.

10.2 *Reference Standards and Calibration Curves and Tables:*

10.2.1 Refer to MNL12 for Thermocouple accuracies.

10.2.1.1 For type K thermocouples, MNL12 specifies the range to be from 0 to 1250 °C (32 to 2300 °F). The "standard tolerance" is ±2.2 °C or 0.75 % of the reading in °C, whichever is greater. The "special tolerance" is ±1.1 °C or 0.4 % of the reading in °C, whichever is greater.

10.2.2 *Discussion on Calibration of DFTs:*

10.2.2.1 Most heat flux gauges (for example, thin film, Gardon, Schmidt-Boelter) are designed to have a linear output with heat flux. Data reduction is easy because the gauge comes with a calibration in the form of a sensitivity coefficient (in other words, xx mV/unit of heat flux), and these sensitivity coefficients are made with reference to a NIST standard.

10.2.2.2 Traditional heat flux gauge calibrations use a radiative only heat source and seek to minimize convection effects (for example, NIST, Medtherm, and so forth). Details of those calibration procedures will not be discussed in detail here. Typical accuracies reported are ±3 %. An effort was initiated at NIST to develop a convective heat transfer calibration capability, but the effort was not completed and no such facility exists at NIST. A convective calibration capability does exist at Virginia Tech University under the guidance of Prof. Tom Diller.

10.2.2.3 A detailed analysis of heat flux gauges has led to a better understanding of under what conditions one can assume the linear sensitivity coefficients are an accurate representation of the behavior of the heat flux gauges. A body of evidence has shown that in fact the sensitivity coefficients developed for radiation only calibrations are not accurate for mixed heat transfer applications where convection is non-negligible. (See references in the Introduction.)

10.2.2.4 For both Gardon and Schmidt-Boelter gauges what has been discovered is that the gauge sensitivity for an equivalent level of radiant heat flux is different than for the same level of convective heat flux. One might reasonably ask: "So what?" How much does this affect readings? These are good questions that will be discussed below. First, a simple example will be discussed to show possible effects of the problem.

10.2.2.5 For a radiation only heat flux measurement, one records the voltage output and multiplies the output by the

sensitivity coefficient provided by the manufacturer to get an estimate of heat flux. This is expressed in Eq 1:

$$q = v \cdot S \tag{1}$$

where:

q = the heat flux,
v = the voltage output, and
S = the sensitivity coefficient (unit of heat flux/volt).

10.2.2.6 What is normally done is the user assumes the sensitivity coefficient is the same for all modes of heat transfer, therefore one estimates the heat flux using Eq 1. But it has been shown that one should not assume the sensitivity coefficients are the same, therefore, a different data reduction method is appropriate. How then does the user reduce his data?

10.2.2.7 One method to reduce the data is to use a linear combination of the fluxes as shown in Eq 2:

$$q = v \cdot (F_{rad} \cdot S_{rad} + F_{conv} \cdot S_{conv}) \tag{2}$$

where:

F_{rad} and F_{conv} = the fractions of the total heat flux attributed to radiation and convection, and
S_{rad} and S_{conv} = the radiative and convective sensitivity coefficients.

10.2.2.8 What makes Eq 2 difficult to use is that most of the terms are not known to high accuracy. Only S_{rad} is known to good accuracy (from the manufacturer); none of the others are known except the output voltage.

10.2.2.9 Eq 2 assumes that both the radiative and convective sensitivity coefficients are linear with heat flux. This is true for radiative flux but it has not been shown the case for convection. But Eq 2 serves to make the point, as follows.

10.2.2.10 In Eq 2, assuming the radiative and convective sensitivity coefficients are equal, and the sum of the radiative and convective fractions equals 1.0, then Eq 2 is reduced to Eq 1. This is in fact what every user of heat flux gauges assumes, whether known or not, when using a calibration performed in radiation only.

10.2.2.11 For Gardon and S-B gauges the convective sensitivity coefficients can be quite different from radiative sensitivity coefficients. For example, Gifford, et al., 2010 (**4, 10**), showed that for S-B gauges the convection sensitivity coefficients can be up to about 20 % different than the radiation sensitivity coefficients. Further complicating matters is that the convective sensitivity coefficients are different for shear and stagnation flows. Similar results have been shown for Gardon gauges by Kuo and Kulkarni, 1991 (**8**).

10.2.2.12 Why would Gardon and S-B gauges have different sensitivity coefficients in radiative and convective environments? A qualitative understanding is possible by understanding how the gauges are constructed. Gardon gauges have a very thin sensing element that has a parabolic temperature profile from the center of the element to the edge when exposed to a uniform radiative heat flux. But during a convective shear flow, the temperature profile can "tilt" to the downstream side of the sensing element. There is good reason to expect that the sensitivity coefficient for a Gardon gauge in shear flow might be different than for the same magnitude of radiative heat flux.

10.2.2.13 Similarly, for S-B gauges, one assumes a uniform exposure of radiative flux over the sensing element. In shear flow this is not the case so again one might expect different sensitivities for radiative and convective fluxes.

10.2.2.14 Therefore, because sensitivity coefficients in radiative and convective heat transfer environments are different when using Gardon and S-B gauges, and there is no NIST traceable convective heat flux calibration capability, and because making an estimate (for example, using Eq 2) of the heat flux in mixed heat transfer environments has a number of uncertain parameters, it is difficult to fully understand the uncertainty of these types of gauges when used in a mixed mode heat transfer environment. Therefore, a different method to estimate heat flux was developed.

10.2.2.15 Characteristics of this "different" method were as follows:

(1) The gauge had to be rugged and survive temperatures up to about 1100 °C.

(2) The gauge should not be actively cooled.

(3) The gauge does not use a single sensitivity coefficient, so one does not suffer from the issues discussed above (different radiative and convective sensitivity coefficients).

(4) The gauge is simple so can be analyzed by means of a thermal model.

(5) The gauge responds to both radiation and convection so one measures the total heat flux to a surface.

10.2.2.16 DFTs satisfy all of the desired characteristics listed above. But the downside is the complication of data reduction and a more complicated uncertainty analysis. The uncertainty analysis for DFTs is more complicated, and depends on the data reduction method used (in other words, energy storage method, inverse heat conduction, inverse filter function).

10.2.2.17 With DFTs, one trades the convenience of having a linear sensitivity coefficient with known and traceable accuracy and a relatively complicated gauge design (S-B and Gardon) for a much simpler design (in other words, DFTs) with a more complicated data reduction and uncertainty analysis.

10.2.2.18 The discussion above sheds light on the advantages of using a gauge that does not require a calibration, assuming one has the tools to reduce the data and analyze the uncertainties when using DFTs.

11. Calculation or Interpretation of Results

11.1 *General:*

11.1.1 The data analysis techniques in this section use the DFT plate temperature histories and material properties to provide quantitative estimates of net heat flux data over the entire test duration. The inverse heat conduction analysis and energy storage methods both calculate the net heat flux post-test. The inverse filter function method provides near real-time estimates of net heat flux during a test.

11.1.2 Implicit in the energy storage method analyses is that the temperature measurements, made on the unexposed side of the plate, are sufficiently close to the exposed side temperature. This is due to the relatively high conductivity of the Inconel plate. The TCs are mounted on the unexposed side because the bias errors are lower and survivability is higher. This assumption can be confirmed with an inverse heat conduction analysis

which provides an estimate of the exposed side plate temperature. The measurements are typically very close to that estimated from inverse heat conduction calculations (see Appendix X5 for an example). This approximation is more accurate for the 1.6 mm plate. The inverse heat conduction method does not suffer from this assumption.

11.1.3 Before the heat flux estimation techniques are described, an energy balance on the sensing surface will be developed, and how one should use the measurement will be discussed.

11.2 *Energy Balance on DFT:*

11.2.1 An energy balance on the surface of a DFT is important to understand how heat flux is estimated. All measurement devices (for example, DFTs, S-B and Gardon gauges) generate a voltage output based on the net energy absorbed into the sensing surface. But in gauges that are calibrated to a known standard (for example, Schmidt-Boelter and Gardon types), the gauge output is calibrated to the source, which is known to high accuracy and is traceable to NIST. Typically Gardon and Schmidt-Boelter gauges are calibrated to an incident heat flux.

11.2.2 The energy balance on any surface (DFT, test item, and so forth) is formulated as follows:

$$q_{net} = q_{inc,r} - q_{refl} - q_{emit} + q_{conv} \quad (3)$$

where:

q_{net} = net heat flux into the surface, which includes both radiative and convective contributions,
$q_{inc,r}$ = incident radiative heat flux, also called irradiance,
q_{refl} = reflected radiative heat flux, fraction of incident radiative heat flux reflected from the surface,
q_{emit} = emitted heat flux from surface, and
q_{conv} = convective heat flux, assumed positive into the surface; q_{conv} is expressed as Newton's Law of Cooling.

11.2.3 The net heat flux (q_{net}) is the absorbed heat flux minus the re-radiated flux. When using DFTs, the net heat flux is what is estimated from an inverse heat conduction analysis or energy storage method. For Gardon and S-B gauges, which are water cooled, the emitted flux is negligible and the convective flux is minimized by a careful design of the calibration apparatus. For Gardon or S-B gauges one normally calibrates the gauge output to the incident flux (any gauge generates an output proportional to the energy absorbed, which is the net flux, but Gardon and S-B gauges are calibrated to the incident flux).

11.2.4 Implicit in Eq 3 is there are no other sources of heat transfer present (for example, condensation).

11.2.5 The first two terms on the RHS of Eq 3 can be combined:

$$q_{inc,r} - q_{refl} = \alpha_{DFT} q_{inc,r} \quad (4)$$

11.2.6 The emitted heat flux can be expressed as follows:

$$q_{emit} = \varepsilon_{DFT} \cdot \sigma \cdot T_{DFT}^4 \quad (5)$$

where:

α_{DFT} = the plate absorptivity, and
ε_{DFT} = the plate emissivity.

11.2.7 Rearranging Eq 3 and assuming $\varepsilon_{DFT} = \alpha_{DFT}$:

$$q_{inc,r} = (q_{net} / \varepsilon_{DFT}) + (\sigma \cdot T_{DFT}^4) + \left[\left(\frac{h}{\varepsilon_{DFT}} \right) \cdot (T_{DFT} - T_{gas}) \right] \quad (6)$$

11.2.8 In Eq 6, one can measure or estimate ε_{DFT} and h. T_{DFT} is measured. T_{gas} can be assumed equal to the fire or flame temperature. If CFD simulations are available, the temperature of the fluid near the DFT can be used for T_{gas}. Because 'h' and T_{gas} are assumed constant, one should consider this a quasi-steady energy balance. q_{net} can be estimated in three ways as discussed next.

11.3 *Inverse Heat Conduction Analysis Method:*

11.3.1 The inverse heat conduction analysis uses a one dimensional, nonlinear, transient thermal model of the DFT [in other words, Beck, J. V., 1985, 1999 (**32, 33**); Blackwell, B., 1987 (**34**)]. Temperature dependent thermal properties are used in this analysis. The inverse heat conduction analysis is used to obtain the net heat flux over the entire test duration. The inverse calculations use a dynamic thermal model of the sensor with the two DFT plate temperature measurements to calculate the net heat flux to the exposed surface. Inverse calculations are performed post-test. Note that the net flux estimated from an inverse heat conduction analysis is not unique. For example the results will change depending on the number of "future times" used during the calculation (the number of future times is an input to the program).

11.3.2 One example of an inverse heat conduction code is "IHCP1D" [Beck, J. V., 1999 (**33**)]. IHCP1D is a nonlinear inverse heat conduction analysis code from Beck Engineering Consultants, Okemos, MI. Another code is called "SODDIT" for Sandia One Dimensional Direct and Inverse Thermal code [Blackwell, B. F., 1980 (**34**)]. Other inverse heat conduction codes can also be used.

11.4 *Inverse Filter Functions (IFF) Analysis Method:*

11.4.1 For a near real time estimate of heat flux one can use Inverse Filter Functions (IFF) [Beck, J. V., 2008 (**35**); Keltner, N. R., 2008 (**17**)]. The IFFs can be programmed into data acquisition systems to cover a furnace temperature range of ambient to 950 °C. The IFFs are copyrighted: they will be provided under license to ASTM for use in ASTM Test Methods. They are specific to a DFT design and construction, require a 1 Hz data acquisition rate, 3 mm thick plates, and provide one second resolution of the heat flux. They have only been developed using IHCP1D. IFFs have not yet been developed for SODDIT. Using data from a Test Methods E119 furnace test, Fig. 4 shows a comparison of the heat flux histories calculated with IHCP1D and the Inverse Filter Functions. As can be seen the agreement is good. In this example, the oscillations in heat flux in the first 700 to 800 s are due to the very slow response of the furnace control thermocouple.

NOTE 1—8 PCF (128 kg/m^3) Cerablanket ceramic fiber insulation from Thermal Ceramics has been used in the development of the inverse filter functions for DFTs. The inverse filter functions are specific to the specified DFT design, the specified plate and insulation materials, and a data sampling rate of 1 Hz (1 s). The data in Annex A1 applies only to the 1 in. thick Cerablanket when it is compressed to 75 % of its original thickness (1.91 cm; 0.75 in.). Any changes in materials, material thicknesses, thermocouple design and attachment method or data sampling rate will invalidate the use of the filter functions.

11.5 *Energy Storage Method:*

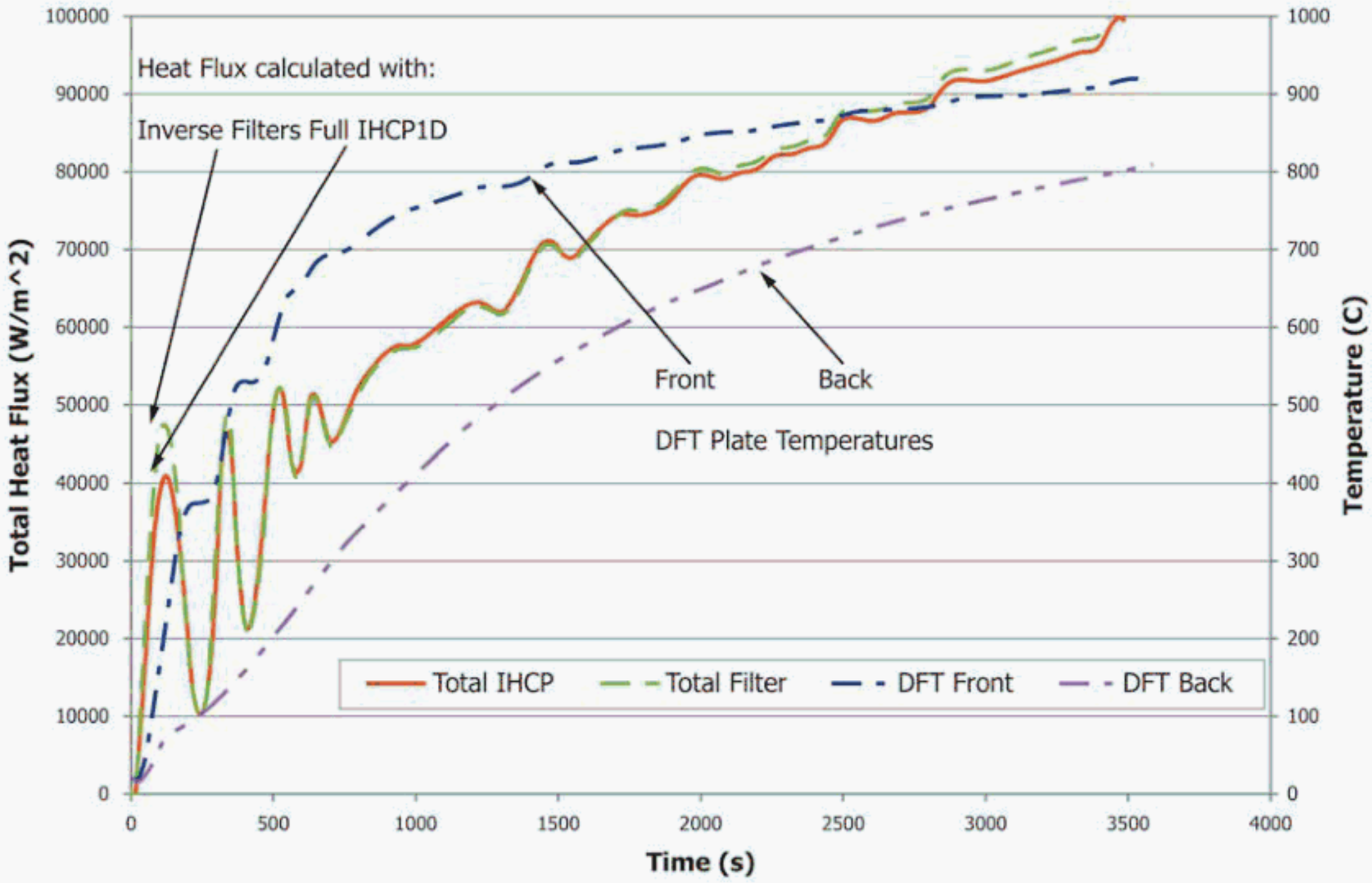

NOTE 1—In Fig. 4, the oscillations in heat flux are due to the very slow response of the furnace control thermocouple. To try to match the Test Methods E119 time temperature curve, the firing is at full power until the measured temperature approaches the curve and then it is shut-off until it falls below. This is sometimes called "bang-bang" control.

FIG. 4 Heat Flux from Inverse Heat Conduction Analysis Compared with Near Real-Time Filter Function Results

11.5.1 The third method to estimate net heat flux is called the "energy storage" method. The governing equation is developed by forming an energy balance on a control volume comprising the DFT plate and the first node in the insulation (see 11.5.4). The net heat flux is the energy stored in the DFT plate plus the energy lost into the insulation (the insulation is not adiabatic, so some energy is lost). See **(36)** and **(37)** for more details on the development of the energy method.

11.5.2 q_{net} can be estimated as follows:

$$q_{net} = \left(\rho_{pl} * C_{p-pl}(T_{pl}) * L_{pl} * \frac{dT_{plate}}{dt} \right) + \left(k_{ins}(x = L_{pl}) * \frac{dT_{insul}}{dx(x = L_{pl})} \right) \quad (7)$$

11.5.3 The first term in Eq 7 is the energy stored in the front (heated) plate and the second term is the energy conducted into the insulation (in other words, energy lost to the insulation). T_{plate} is the TC measurement on the back of the front (that is, heated) plate, and T_{insul} is the insulation temperature at the first node inside the insulation next to the front plate. T_{insul} is calculated separately, as shown in the next section. $dT_{insul}/dx(x=L_{pl})$ is estimated by taking the difference between the plate temperature (T_{plate}) and the insulation temperature at the first node in the insulation and dividing by the node dimension (Δx). See 11.5.4 for the method to calculate the insulation temperature. k_{ins} is the conductivity of the insulation; ρ_{pl} and $C_{p\text{-}pl}$ are material properties of the plate. L_{pl} is the DFT plate thickness. A spreadsheet can be used to solve Eq 7. Assuming one has the correct temperature dependent thermal properties Eq 7 is a transient estimate of q_{net}. Thermal properties of 304SS and the Cerablanket insulation (see Annex A1) were used in Eq 7. Fig. 5 and Fig. X5.2 in Appendix X5 show a comparison of net heat fluxes generated from an inverse heat conduction analysis and the energy storage method. As can be seen the agreement is very good.

11.5.4 The second term in Eq 7 is calculated using the temperature dependent thermal conductivity of the insulation at the backside of the front plate ($x=L_{pl}$) and the temperature gradient at the boundary between the back side of the plate and the insulation. A simplified analysis of 1-D conduction through the insulation was used to estimate the temperature gradient through the insulation. The two plate temperatures were used as boundary conditions for the insulation and 1 dimensional conduction through the insulation was assumed. Contact resistance is assumed to be negligible, but temperature-dependent conductivity was included. The explicit form of the equation used to make this calculation comes from **(38)**:

$$T_x^{t+\Delta t} = Fo * (T_{x+\Delta x}^t + T_{x-\Delta x}^t) + T_x^t * (1 - 2 * Fo) \quad (8)$$

where:

Fo = the Fourier number $(\Delta t * k)/(\rho * c_p * \Delta x^2)$.

For stability, the Fourier number has to be less than 0.5. Strictly speaking, Eq 8 applies to cases with constant thermal properties, which is not the case here. To partially account for changing properties, the Fourier number was updated at each location and time step in the explicit formulation. Because the

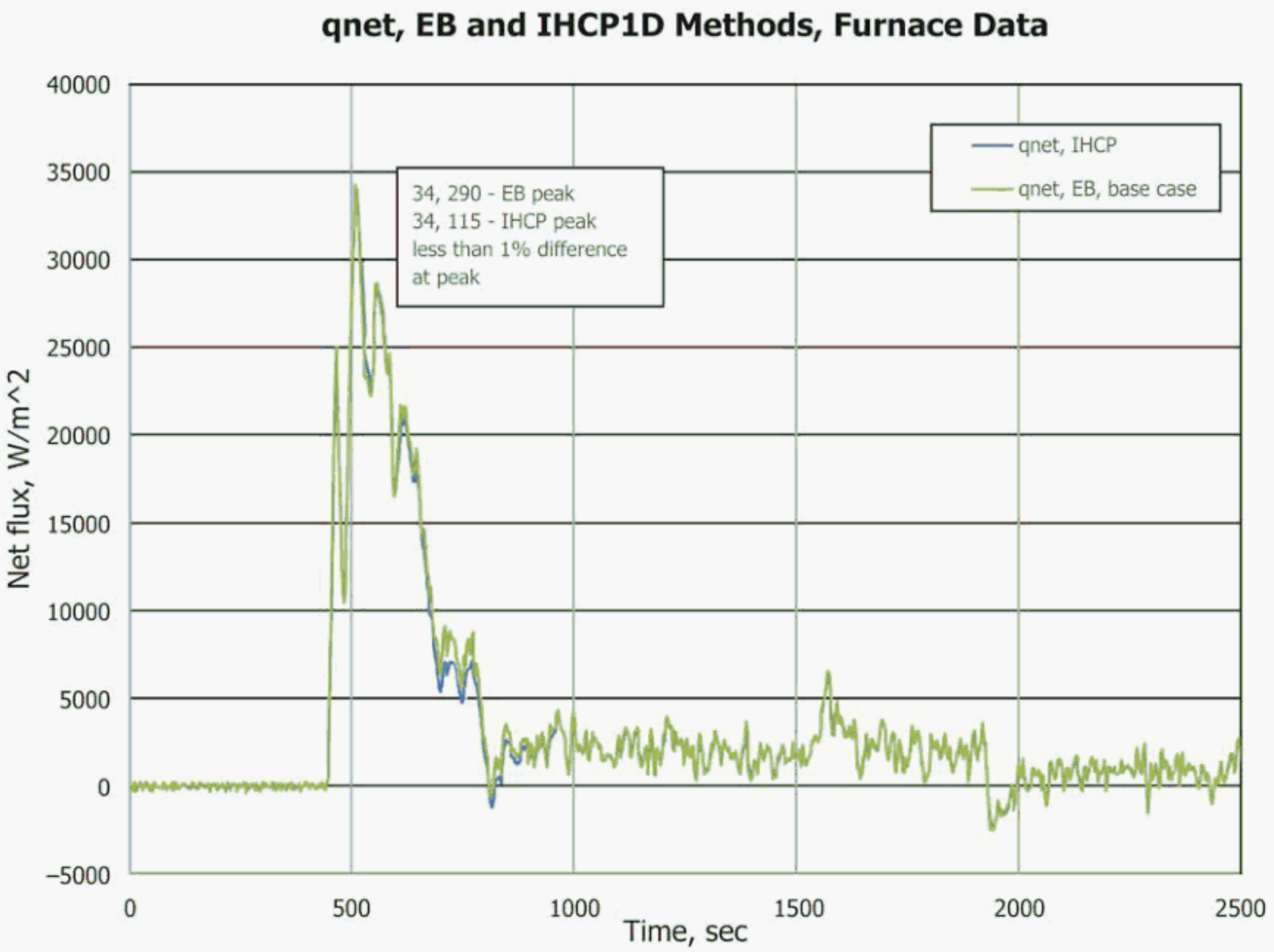

FIG. 5 Comparison of Heat Flux from the IHCP1D and Energy Storage Method

second term in Eq 7 is small compared to the plate storage term, using Eq 8 was sufficient for our purposes.

11.5.4.1 Fig. 5 shows results of the calculations for one of the data sets analyzed (furnace data). It is evident that both methods (inverse heat conduction and energy storage) show almost the same net flux for the entire test. This provides more confidence in the methods.

11.6 *Simplified Early and Late Time Estimations of Heat Flux:*

11.6.1 Appendix X4 describes how one can estimate approximate values for early and late time heat fluxes and incident radiative flux. These calculations are valuable but optional, so they are provided in the appendix.

11.6.2 For early times (no more than 5 min), a modification to the Thin-Skin Calorimeter approximation involves using an estimate of the heat transfer (loss) into the insulation layer to calculate the net heat transfer to the front plate (see Test Method E459).

11.6.3 After the first 10 to 15 min in a furnace test (in other words, "later times"), heat transfer through the DFT is in a quasi-steady state condition. As a result, the temperatures of the front and back plates are rising at essentially the same rate. The late time analysis calculates the heat transfer through the DFT plus the energy storage in the plates and insulation. Using an energy balance for the DFT Front Plate, an "Effective Furnace Radiation Temperature" (EFRT) can be calculated [Keltner, N. R., 2007 (**16**)]; this is the blackbody temperature that would produce the same total heat flux exposure. The EFRT calculation accounts for energy storage in the plates from radiation and convection, transmission through the insulation layer and heat loss (re-radiation) off the front face and off the back face of the DFT to the test assembly.

11.7 *Example:*

11.7.1 Appendix X5 provides an example of how these various methods can be applied to a furnace test and provides several other useful calculations as listed below:

11.7.1.1 Simplified early time heat flux calculations, X4.1.

11.7.1.2 Simplified later time heat flux calculations, X4.2.

11.7.1.3 Simplified very late time heat flux calculations, X4.3.

11.7.1.4 Incident heat flux calculations.

11.7.1.5 Thermal penetration and communication times.

12. Report

12.1 A report should be written documenting all aspects of the experiment. An uncertainty analysis is highly recommended because the accuracies of net heat flux from DFTs are application dependent. See 10.2.2.

13. Precision and Bias

13.1 *Statements of Precision and Bias*—Precision and bias statements apply to test methods that will generate the same results. This DFT test method will generate different results during each test because each test will be different. The precision of the result depends on the calibration of the DAS. The bias of the result depends on the user's ability to install the

thermocouples correctly and to understand the potential biases in the data reduction method chosen. More detail is provided in the next section, Measurement and Uncertainty, and in 10.2.2.

14. Measurement and Uncertainty

14.1 The accuracies of incident heat flux reported for commercially available Schmidt-Boelter and Gardon gauges are typically ±3 % of the reading. This accuracy applies only to the calibration configuration, which seeks to minimize the convective contribution to the gauge during calibration. If one were to use the gauges in exactly the same manner as they were calibrated, then one could use the ±3 % accuracy value with confidence. An estimate of the total uncertainty of Gardon gauges in real applications (versus in the calibration laboratory) is provided Test Method E511-07: "The consensus on application uncertainty was four to six times the calibration uncertainty" (the calibration uncertainty is typically ±3 %).

14.2 Real fire tests, however, are not the same as the carefully controlled calibrations. Real fires have some level of convection (for example, from wind driven fires in the outdoors, to fires indoors with complicated ventilation flows). Uncertainties in the estimation of incident heat flux (not net flux) are provided in Bryant, et al., 2003 (**39**) for a room fire and Nakos, J. T., 2005 (**40**) in pool fires. They are much higher than typically assumed (for example, ±21 – 42 % to 95 % confidence in Nakos, 2005 and ±7 – 25 % to 67 % confidence in Bryant, et al., 2003). This analysis assumes a significant convective component.

14.3 An uncertainty estimate for inverse heat conduction methods ranged from 15 to 19 % for a 95 % confidence level [Figueroa, V. G., 2005 (**26-28**)]. Based on the 5 to 10 % changes used for parameters such as the thickness of the Inconel plates, which can be measured accurately, these estimates are conservative.

14.4 An uncertainty estimate for DFTs ranged from 12 to 15 % [Keltner, 2008 and 2010 (**16, 17**)]. This is comparable to the uncertainties listed in 14.2 above. The bias error has not been determined for the furnace DFT because biases for heat flux measurements are test dependent. DFT uncertainty estimates should be made on a case by case basis because convection can be a large contributor to the overall uncertainty, and convection varies from test to test.

14.5 Janssens, M., 2007 (**18**) found agreement within a few percent between a water-cooled Schmidt-Boelter gauge and a DFT in a Test Methods E119 fire resistance test when bare bead thermocouples were used to provide gas temperatures for estimating the effects of convective heat transfer.

14.6 Complicating the response of Gardon and Schmidt-Boelter gauges is that the sensitivity coefficient measured during radiative only calibrations are not the same as for mixed heat transfer or pure convection [Gifford, A., Hoffie, A., Diller, T., and Huxtable, S., 2010 (**10**); C. H. Kuo and A. K. Kulkarni, 1991 (**8**); G. J. Borell and T. E. Diller, 1987 (**3**)]. Therefore, when one reduces data from real fire tests, where there is both a radiative and convective contribution, the uncertainty of the result can be much higher [Nakos, J. T., 2005 (**40**)].

14.7 One benefit of DFTs is that they do not use a calibration sensitivity, and therefore data reduction does not suffer from increased uncertainties that could occur because the sensitivity coefficient was for radiative heat transfer only, or changed during the test (for example, due to convective heat transfer or surface fouling).

14.8 It is highly recommended that the user perform a preliminary uncertainty analysis of the net heat flux before this method is used to be confident the method will provide sufficiently accurate results for their application. References that can help are Keltner, 2010 (**17**); Figueroa, 2005 (**26-28**); Nakos, 2005 (**40**); and Janssens, 2007 (**18**).

15. Keywords

15.1 convective heat flux; directional flame thermometers (DFTs); energy storage method; heat flux measurement; incident heat flux; inverse filter function method; inverse heat conduction method; MIMS (mineral insulated, metal sheathed); net heat flux; thermocouple (TC)

ANNEX

(Mandatory Information)

A1. TEMPERATURE DEPENDENT THERMAL PROPERTIES FOR USE IN HEAT FLUX CALCULATIONS

A1.1 The energy storage calculations and inverse heat conduction analysis in this standard are based on using Inconel 600 and compressed Cerablanket insulation when building Directional Flame Thermometers. These thermal properties are not valid for other materials. Values at temperatures between those provided are linearly interpolated if the property variation with temperature is close to linear. For those property values that are not close to linear, one can generate an appropriate curve fit to the data, which can be used for interpolating. Density values are multiplied by the specific heat to obtain the volumetric heat capacity.

NOTE A1.1—The thermal conductivity for the insulation shown in the following tables is the local conductivity; it is not the effective conductivity (Test Method C177) typically shown in the insulation manufacturer's literature. If other ceramic fiber insulation is used in place of Cerablanket, the Inverse Filter Functions developed for a DFT fabricated

with the Cerablanket will be in error due to different thermal properties. If other insulation materials are used, the initial density of the insulation layer, the actual thermal conductivity and the specific heat as functions of temperature, and the change in thermal conductivity for any compression are required for accurate analysis of heat flux exposures using an inverse heat conduction code.

TABLE A1.1 Temperature Dependent Thermal Properties of Inconel 600

Thermal Conductivity Table			
Temperatures for thermal conductivity (°C)			
25	127	527	727
Components of thermal conductivity (W/m-°C)			
14.9	16.6	22.6	25.4

Volumetric Heat Capacity Table			
Temperatures for volumetric heat capacity (°C)			
25	127	527	727
Components of volumetric heat capacity (J/m^3-°C)			
3 768 000	4 068 500	4 598 000	4 827 000

TABLE A1.2 Temperature Dependent Thermal Properties of Compressed Cerablanket

Thermal Ceramics—8 lbs/ft^3 Cerablanket—Compressed 25 %

Thermal Conductivity Table				
Temperatures for thermal conductivity (°C)				
35	238	516	765	855
Components of thermal conductivity (W/m-°C)				
0.047	0.072	0.125	0.205	0.244

Volumetric Heat Capacity Table				
Temperatures for volumetric heat capacity (°C)				
23	250	500	750	1000
Components of volumetric heat capacity (J/m^3-°C)				
145 900	169 400	185 700	200 200	210 900

APPENDIXES

(Nonmandatory Information)

X1. APPLICATIONS USING DFTs

X1.1 Testing Applications

X1.1.1 Although DFTs have been used in a wide variety of fires, many of the applications described below are related to quantitative heat flux measurement results in fire resistance tests.

X1.1.2 *Net Heat Flux Exposure,* during the fast temperature ramp (first 5 min) using three DFT-like sensor designs with three different response times; the three net heat flux measurements generally agreed within a couple percent over the first 250 s before the thinnest one rolled off due to its faster temperature rise; these results demonstrate that the dynamic response characteristics of the three DFT-like designs are not very important at early times [Keltner, 2008 (**17**)].

X1.1.3 *Net Heat Flux to A Test Unit,* with a metal surface over the entire test duration; there was very good agreement between estimates made using DFT data and those calculated for the metal test unit with a nonlinear inverse heat conduction code [Keltner, N. R., 2002 (**41**)].

X1.1.4 *The Heat Flux in Real-time,* using the new Inverse Heat Conduction/Digital Filter Function technique; agreement between a full nonlinear inverse heat conduction analysis and the inverse filter function calculations was very good over an hour long-test, except for the first peak, which occurred about 100 s after ignition, in an oscillating signal [Beck, J. V., 2008 (**35**); Keltner, N. R., 2008 (**17**)]. See Fig. 4 in the main body of this test method.

X1.1.5 *Cold Wall Heat Fluxes*—Janssens, M., 2007 (**18**), at the Southwest Research Institute, presented a comparison of methods for measuring thermal exposure in fire resistance tests at the ISO Workshop on Heat Transfer Calculations and Measurements in Fire Safety Engineering–Furnace Characterization and Control. It showed very good agreement between cold-wall heat fluxes measured with water-cooled, Schmidt-Boelter heat flux sensors and those calculated from DFT heat fluxes and gas temperatures measured with bare-wire thermocouples. The heat flux levels estimated from Plate Thermometer temperature histories were lower than the Schmidt-Boelter or DFT values.

X1.1.6 *Net Heat Flux to A Test Unit*—In a project sponsored by the US Coast Guard using IMO A754 marine fire resistance test methods, the Test Methods E457 and E459 approaches along with an advanced thin-skin technique [Carslaw and Jaeger, 1959 (**42**)] were used for DFTs with 1.6 or 3.2 mm thick Inconel face plates. The test unit was called the "Furnace Characterization Unit" (FCU) and it was designed to simulate a marine bulkhead. The analysis showed peak heat flux exposures of 30 to 40 kW/m^2 in vertical furnaces and 25 to 30 kW/m^2 in horizontal furnaces [Keltner, N. R., 2002, 2007 (**16, 41**)]. The non-linear, inverse heat conduction analysis code (IHCP1D) was used to calculate the net heat transfer rates to the front face of the various DFTs as well as to the large, actively cooled, FCU over test durations of up to one hour. The inverse calculations showed good agreement with the total heat fluxes calculated with the simplified, early, and late time DFT analysis techniques. In a wall furnace test, measurements made with the two different DFT designs and the FCU showed integrated total heat flux exposures over one hour differed by less than 3 %.

X1.1.7 In the 2008 ASTM E5 Symposium, Keltner, N. R., et al., 2002, 2007 (**16, 41**) showed a comparison of the net heat flux to the FCU calculated with the IHCP1D inverse heat conduction code [Beck, J.V., 1999 (**33**)] using three, in-depth FCU temperature measurements with the heat flux calculated from the DFT net heat flux and the DFT hot-face and FCU surface temperature measurements. From the DFTs and the FCU measurements, the paper also showed the total heat flux exposures calculated by adding reradiation to the net heat flux. For the two approaches, the integrated total heat fluxes differed by less than 1 % over the nearly hour-long test.

X1.1.8 In the 2008 ASTM E5 Symposium, Sultan, M., 2008 (**23**) demonstrated the differences between the furnace temperature control sensors (Test Methods E119 Shielded Thermocouple, ISO 834 Plate Thermometer, Test Methods E1529 Directional Flame Thermometer and bare, beaded thermocouple). The paper demonstrated that changing the furnace control sensor resulted in different thermal exposure during the test. The differences were largest during the initial fast ramp, when the measured heat flux varied by more than 100 % between the various sensors.

X1.1.9 From a horizontal furnace test with an uninsulated steel ceiling, a total heat flux exposure of 102 kW/m^2 was calculated from measurements made with the DFTs at 25 min after ignition. Based on this heat flux, the effective furnace radiation temperature was 885 °C [Keltner, N. R., 2007, 2008 (**16, 17**); Sultan, M., 2006 (**22**)]. The estimated thermal exposure (heat flux) based on other temperature measurements were all lower, the DFT Front Face 840 °C (estimated heat flux – 18 % low), ISO-834 Plate Thermometer 824 °C (25 % low), and Test Methods E119 Shielded Thermocouple 787 °C (44 % low).

X1.1.10 In the same furnace with an insulated ceiling, the total heat flux exposure based on measurements made with the DFTs was 79 kW/m^2 (effective furnace radiation temperature of 805 °C); this is 22 % lower than the uninsulated case. The estimates of thermal exposure based on other temperature measurements were all close: DFT Front Face 794 °C (4 % low); ISO 834 Plate Thermometer 812 °C (3 % high); and, Test Methods E119 Shielded Thermocouple 796 °C (3 % low).

X1.1.11 A 2008 ASTM paper showed a comparison of the total heat flux measurements from five IMO A754 fire resistance tests run in four different furnaces lined with ceramic fiber insulation [Keltner, N. R., 2008 (17)]. Although all are controlled to the same time temperature curve using the same temperature sensor, the coefficient of variance (standard deviation/mean) of the total heat flux values starts out in the 20 to 30 % range. From 10 min after ignition to the end of the test, it is approximately 10 %.

X1.1.12 Heat flux measurements made with DFTs have been used to support the development of engineering models [Keltner, N. R., et al., 1994 (43); Noravion, H., et al., 2008 (44)].

X1.1.13 Heat flux measurements have been used in "rapidly deployable instrumentation packages in wild-land-urban fires [Manzello, S. L., 2010 (45)].

X2. EXAMPLE INVERSE HEAT CONDUCTION ANALYSIS

NOTE X2.1—This is an Appendix if any inverse heat conduction code is used, because there are other 1-dimensional heat conduction codes available other than IHCP1D. But it should be considered an Annex if the inverse filter function method is used, because the IFF method was developed using only IHCP1D.

X2.1 This inverse heat conduction analysis was performed for data developed in a test of the Furnace Uniformity Fixture developed for Test Methods E119 using the IHCP1D inverse code.

TABLE X2.1 Example Inverse Heat Conduction Analysis

Beck Engineering Consultants Company
1935 Danbury West
Okemos, MI 48864

Program output file name:
c:\IHCP1D\DFTS fire\Test2 SS interp 2FT corrected.ihc

Temperature measurement input file name:
C:\IHCP1D\DFTS fire\BobBerhinig Test #2,SS interp.txt

Date: 3/3/2008
Time: 1:08:07 PM

Heading:
DFT E119 Furnace Test interpolated data at 10 seconds

**** Step1: Define the GEOMETRY of the experiment. ********************

Main Geometry

Flat plate	Cylindrical radial	Spherical radial
(*)	( )	( )

Units

W-kg-m-sec-°C	cal-gm-cm-sec-°C	BTU-lb-ft-hr-°F
(*)	( )	( )

Number of regions
3

Region material number

1	2	1

Thickness of region (m)

0.00301	0.019	0.00301

Number of nodes per region

2	10	2

**** Step 2: Define QUANTITIES for time steps and regions. ********************

Number of calculated time steps per measured time step
10
Number of time intervals with various future time steps
1
Time at end of interval
3590
Number of future time steps
2

**** Step 3: Define BOUNDARY conditions. ********************

Unknown boundary location

x=0	x=L	Both x=0 and x=L
(*)	( )	( )

Known boundary type

Insulated	Prescribed non-zero heat flux	Prescribed temperature history
( )	( )	(*)

**** Step 4: Describe input DATA file structure. ********************

Number of columns of data
1
( ) Print the data for each sensor
Interface number for input file column
1

**** Step 5: Define temperature-dependent thermal PROPERTIES. ********************

MATERIAL NUMBER 1

Number of components of the thermal conductivity table
4
Number of components of the volumetric heat capacity
4
Thermal conductivity table
Temperatures for thermal conductivity (°C)

25	127	527	727

Components of thermal conductivity (W/m-°C)

14.9	16.6	22.6	25.4

Volumetric heat capacity table
Temperatures for volumetric heat capacity (°C)

25	127	527	727

Components of volumetric heat capacity (J/m^3-°C)

3 768 000	4 068 500	4 598 000	4 827 000

TABLE X2.1 *Continued*

```
        MATERIAL NUMBER 2
Number of components of the thermal conductivity table
        5
Number of components of the volumetric heat capacity
        1
Thermal conductivity table
Temperatures for thermal conductivity (°C)
        35              238             516             765             855
Components of thermal conductivity (W/m-°C)
      0.047           0.072           0.125           0.205           0.244
Volumetric heat capacity table
Temperatures for volumetric heat capacity (°C)
        35
Components of volumetric heat capacity (J/m3-°C)
          170 000

**** Step 6: Define ADVANCED features. ********************
                ( ) Calculate unknown heat transfer coefficient
                Fin effect
                        Insulated sides                 Side heat loss/gain
                              (*)                             ( )

**** Heat Flux Results *********************************************
-----------------------------------------------------
                PROGRAM IHCP1D
                Version 7.1 – NOVEMBER 1999
                Beck Engineering Consultants Company
                Ph: 517-349-6688
-----------------------------------------------------
                CALCULATED INITIAL TEMPERATURE DISTRIBUTION
                23.63   23.63   23.63   23.63   23.63   23.63   23.63   23.63
                23.63   23.63   23.63   23.63   23.63   23.63   23.63

                ESTIMATED RESULTS:
                RESIDUAL = MEASURED TEMP. – CALCULATED TEMP.
                TIME, IN SECONDS
                HT. T. COEF = HEAT TRANSFER COEFFICIENT, IN W/m2-K
                SURFACE T = SURFACE TEMPERATURE AT "UNKNOWN SURFACE", IN CELSIUS OR KELVIN
                ALL OTHER TEMPERATURES ARE IN CELSIUS IF SURFACE TEMPERATURE IS IN CELSIUS
                RESID(I) = RESIDUAL IS IN EITHER CELSIUS OR KELVIN
                HT. FLUX = HEAT FLUX, IN W/m2
                TIME    SURFACE q       SURFACE T       EXP. T(1)       CAL. T(1)       RESID(1)        HT. FLUX(1)     HT. FLUX(L)
                20.00   3445.9          26.84           25.82           26.48           -0.66           112.92          601.28
                30.00   5424.3          31.61           29.74           31.05           -1.3            200.68          -165.05
                40.00   8533.6          39.06           36.27           38.17           -1.9            341.25          -1289.60
                50.00   12756.          50.08           46.27           48.75           -2.5            532.66          -2810.78
                60.00   17986.          65.38           60.60           63.54           -2.9            779.70          -4748.85
                70.00   23521.          85.02           79.81           82.64           -2.8            1061.3          -6911.76
                80.00   28625.          108.37          103.15          105.52          -2.4            1351.3          -8573.87
                90.00   32908.          134.52          129.54          131.32          -1.8            1629.3          -9514.81
                100.00  36071.          162.47          157.92          159.03          -1.1            1881.2          -9710.95
                110.00  37726.          191.15          187.19          187.62          -0.43           2097.1          -9147.38
                120.00  38103.          219.57          216.30          216.07          0.23            2267.0          -7803.59
                130.00  37387.          246.91          244.26          243.54          0.72            2389.5          -5860.31
                140.00  35791.          272.57          270.50          269.39          1.1             2466.6          -4168.76
                150.00  33393.          296.01          294.55          293.07          1.5             2498.6          -2925.11
                160.00  30252.          316.73          315.91          314.09          1.8             2502.5          -2177.15
                170.00  26342.          334.26          334.12          331.97          2.2             2456.9          -1896.34
                180.00  21753.          348.19          348.70          346.29          2.4             2359.7          -2113.02
                190.00  17014.          358.54          359.36          357.02          2.3             2232.8          -2711.32
                200.00  12669.          365.70          366.58          364.53          2.0             2091.0          -3266.89
                (Remainder of data not shown.)
```

X3. TEMPERATURE MEASUREMENT CONSIDERATIONS FOR DFTs

X3.1 To obtain the proper dynamic response when using DFTs, an effective "rule-of-thumb" is the diameter of sheathed TC must be less than or equal to plate thickness. When using a 1.6 mm sheathed TC installation on a 1.6 mm thick 304 stainless steel plate, experiments showed an empirically derived time constant of 1.9 ± 0.05 s for this thermocouple installation [Heinonen, E. W., 1992 (**46**)]. For a DFT with a 3 mm plate, the TC response would be the same (since they are the same size), but the DFT response would be slower.

X3.2 MIMS thermocouples (mineral-insulated, metal sheathed) are subject to a temporary failure phenomena known as "shunting" [Gill, W., and Nakos, J., 1999 (**47**)]. The electrical resistivity of the compacted ceramic insulation (for example, magnesium oxide, MgO) decreases as the temperature increases. Temporary shunting occurs when the electrical resistance between the thermocouple wires drops to a low value. For example, 1.6 mm OD Inconel sheathed, Type K or Type N thermocouples insulated with less than the highest purity magnesium oxide insulation have demonstrated shunting failures at temperatures in the 900 to 950 °C range (see Section 2, MNL12). The failure temperature increases for larger thermocouple diameters. Shunting can be reduced or eliminated by insulating the MIMS TC wires as they exit the DFT, and by specifying the highest purity MgO insulation.

X3.3 For the Test Methods E1529 high-rise or hydrocarbon-curve fire resistance test, the furnace temperature is controlled with 6.4 mm OD (1 mm wall), Inconel sheathed MIMS TCs. The dynamic response of this MIMS TC is between that of the Plate Thermometer and the Test Methods E119 Shielded Thermocouple. In Test Methods E1529, heat flux measurements are made with DFTs of the furnace DFT design. The dynamic temperature response of front plate of this DFT is similar to the Test Methods E119 Shielded Thermocouple response [Janssens, M., 2007 (**18**)].

X3.4 Reed, 1996 (**30, 31**) has shown that for Type K TCs, the process of calibrating the TC changes the wire calibration above about 320 °C. It is therefore prudent to purchase a few additional TCs and use them only for calibration purposes. Then, if the calibrated TCs meet ASTM standards for Type K TCs (in other words, ±2.2 °C or ±0.75 % of the reading, whichever is greater), one can reasonably conclude that other TCs made from the same batch of wire also will meet the ASTM standards.

X4. SIMPLIFIED EARLY AND LATE TIME ESTIMATIONS OF HEAT FLUX

X4.1 Simplified Early Time Heat Flux Calculations (Time <5 min; Applies to Furnace Tests)

X4.1.1 The net heat flux during the early part of a typical furnace test (time <5 min) can be estimated from the Furnace DFT front plate (furnace side) temperature measurements using Test Method E457-2002 Standard Test Method for Measuring Heat-Transfer Rate Using a Thermal Capacitance (in other words, Slug) Calorimeter or Test Method E459-2005 Standard Test Method for Measuring Heat-Transfer Rate Using a Thin-Skin Calorimeter (see Section 2). The net flux is estimated from the first term in Eq 7; the second term in Eq 7 is assumed to be zero since we assume a perfectly insulated back side. The slug calorimeter approximation is equal to the first term in Eq 7. To minimize re-radiation effects, the temperature rise should be limited to about 250 to 300 °C.

X4.1.2 A modification to the slug calorimeter approximation involves using an estimate of the heat transfer (loss) into the insulation layer to calculate the net heat transfer (therefore, non-adiabatic insulation is assumed on the back side). Heat loss from the plate into the compressed Cerablanket insulation layer was approximated using a model for a high thermal conductivity plate in contact with a very thick layer of insulation [Carslaw, H. S., et al., 1959 (**42**)]. Using an Inconel plate thickness of 3 mm with the thermal conductivity and volumetric heat capacity (density · specific heat) of both the Inconel and Cerablanket evaluated at roughly the midpoint temperature (250 to 275 °C), an analysis showed the slope of the plate temperature versus time was approximately 90 % of the slope when the unexposed surface of the plate was assumed to be adiabatic (in other words, no heat loss into the insulation). Therefore, a 0.9 correction factor is used to modify the slug calorimeter flux for 3 mm thick plates. Based on Keltner, 2009 (**48**), this same correction factor can be applied to the 1.6 mm thick plate with good accuracy.

X4.1.3 The heat capacity of the plate (volumetric heat capacity · thickness) is approximately 4,333,000 · .003 = 13000 kJ/m^2 K (see Table A1.1, Annex A1). The emissivity or absorptivity is assumed to be about 0.85. Then for the DFT plate:

$$\text{Net heat flux } (t) \approx 13000 \cdot (\Delta T / \Delta t) / 0.9 \qquad \text{(X4.1)}$$

X4.2 Simplified Later Time Heat Flux Calculations (Time > 10 to 15 min; For Furnace Tests)

X4.2.1 After approximately the first 15 min in a furnace test (in other words, "later times"), heat transfer through the DFT is in a quasi-steady state condition; in other words, the temperatures of the front and back plates are rising at essentially the same rate. As a result, the late time analysis calculates the heat transfer through the DFT using the temperature dependent thermal conductivity of the ceramic fiber insulation layer that separates the two Inconel plates. In addition to the heat transfer through the DFT, the late time analysis also calculates energy storage in the plates. This heat transfer is used as part of an energy balance analysis on the DFT sensing plate.

X4.2.2 Using an energy balance for the DFT Front Plate, an "Effective Furnace Radiation Temperature" (EFRT) can be calculated [Keltner, N.R., 2007 (**16**)]; this is the blackbody temperature that would produce the same total heat flux exposure. The EFRT calculation accounts for energy storage in the plates from radiation and convection, transmission through the insulation layer and heat loss (re-radiation) off the front face and off the back face of the DFT to the test assembly. As a result, it provides a more accurate measure of late time thermal exposure than estimates made from individual temperature measurements such as the ISO 834-1 Plate Thermometer or the Test Methods E119 Shielded Furnace Thermocouple.

X4.2.3 The "thermal exposure" is a convenient measure of the total heat flux onto a unit under test. It is defined (see Section 3, Terminology) as the sum of the incident radiative flux and the convective flux. For late times, the convective heat flux is small so the thermal exposure can be estimated as follows:

$$Thermal\ Exposure = q_{inc,r} = \varepsilon_{eff} \times \sigma \times T^4_{Effective} \quad (X4.2)$$

$T_{Effective}$ can be calculated as follows (see Eq 4):

$$\varepsilon_{eff} \times (\sigma \times T^4_{Effective}) = q_{net}/\alpha_{DFT} + (\sigma \times T^4_{DFT}) \quad (X4.3)$$

ε_{eff} is assumed to be equal to 1.0, see section 11.6.3.

$$T_{Effective} = ((q_{net}/(\sigma \cdot \alpha_{DFT})) + T^4_{DFT})^{1/4} \quad (X4.4)$$

As can be seen, unless q_{net} is less than zero, $T_{effective}$ is always greater than T_{DFT}.

X4.2.4 The Adiabatic Surface Temperature (AST) is a similar estimate obtained from the temperature measurement history of a Plate Thermometer [Wickstrom, U., 1997 (**49**)]. Because the EFRT calculation accounts for heat transfer through the insulation and heat loss off the back surface, it provides a more accurate estimate of the thermal exposure than the AST technique.

X4.2.5 For times greater than 10 to 15 min, the thermal exposure provides a good estimate of the incident heat flux to the DFT because the convective contribution is negligible. It can be calculated from the EFRT ($T_{Effective}$) with the flame emissivity assumed to equal 1.0, because $T_{Effective}$ is an effective blackbody temperature.

X4.3 Simplified Very Late Time Heat Flux Calculations

X4.3.1 At very late times, the DFT has either equilibrated with the fire so T_{DFT} is constant, or T_{DFT} is only slowly rising. The convective heat flux is negligible because the DFT temperature and local temperature are close. The net heat flux is low because (a) the plate temperature is not changing, or is changing slowly, and (b) the temperatures of the front and back plates are very close. If both of these conditions are met, then the incident heat flux to the DFT can be approximated by using Eq 6, simplified to the following:

$$q_{inc,r} = \sigma \cdot T^4_{DFT} \quad (X4.5)$$

X4.4 Incident Heat Flux Calculations

X4.4.1 At any time during the test the incident heat flux can be estimated by use of Eq 6. q_{net} is estimated by either the inverse heat conduction or energy storage methods, and ε_{DFT} is measured before and after the test. The convective heat transfer coefficient *'h'* is estimated from correlations; in fire applications, appropriate *'h'* values have been documented in Nakos, 2005 (**40**). T_{gas} is typically measured using shielded TCs.

X4.5 Thermal Penetration and Communication Times

X4.5.1 Approximate thermal penetration times for compressed Cerablanket:

(1) 7 s at room temperature

(2) 3.6 s at 500 °C

(3) 2.1 s at 850 °C

Thermal Communication Time = 4 · Thermal Penetration Time.

X5. EXAMPLE

X5.1 The following example will serve to show how the various methods are implemented. Data from a DFT in a furnace test was used. Data is from Omega Point Laboratories (OPL) and is designated test "OPL#1."[9]

X5.1.1 The DFT was made from 1.6 mm thick 304 stainless steel plates (not Inconel 600, in this case). The same compressed ceramic fiber insulation as shown in Fig. 4 was used. The test was controlled using a furnace TC and used the ISO 834 temperature curve as the desired furnace temperature vs time curve. Fig. X5.1 shows the temperature plot of the DFT ("EXP. T(1)") and the desired ISO 834 curve.

X5.1.2 The DFT was mounted vertically in a Side-Fired, Vertical (Wall) Furnace. These furnaces are much taller and wider than they are deep.

X5.1.3 Using properties for 304 SS and Cerablanket insulation, the net heat flux was estimated using IHCP1D and the energy storage method; results are shown in Fig. X5.2. As can be seen, the net heat flux is high early in the test as the temperature rises, but drops quickly (~700 to 800 s into the test) to almost zero, because the DFT is approaching the furnace temperature, so the net flux absorbed into the DFT is low. Remember that the flux calculated from the inverse and energy storage method both apply to the entire test, not just the early or late parts. Agreement between the two methods is very good throughout the test.

X5.1.4 Eq 7 (first term, slug approximation) and Eq X4.1 (see 11.5 and Appendix X4) were used to estimate the early time net heat flux. Results are shown in Fig. X5.3. As can be seen, the agreement between the IHCP1D net flux (red), the net flux from the slug approximation (purple) (Eq 7, first term), and the slug approximation adjusted using the 0.9 factor (blue)

[9] Use of these data is gratefully acknowledged.

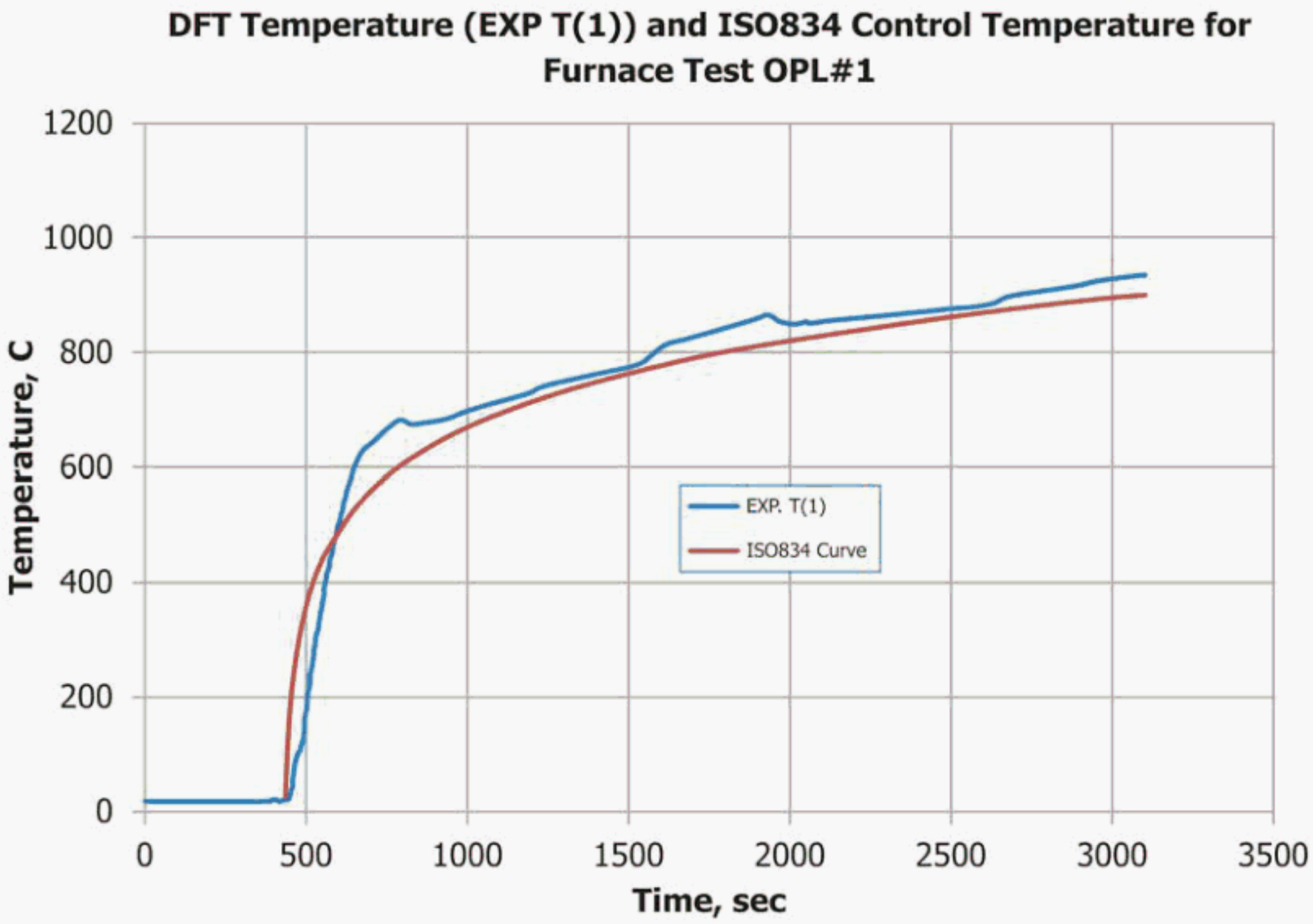

FIG. X5.1 DFT and ISO 834 Temperatures

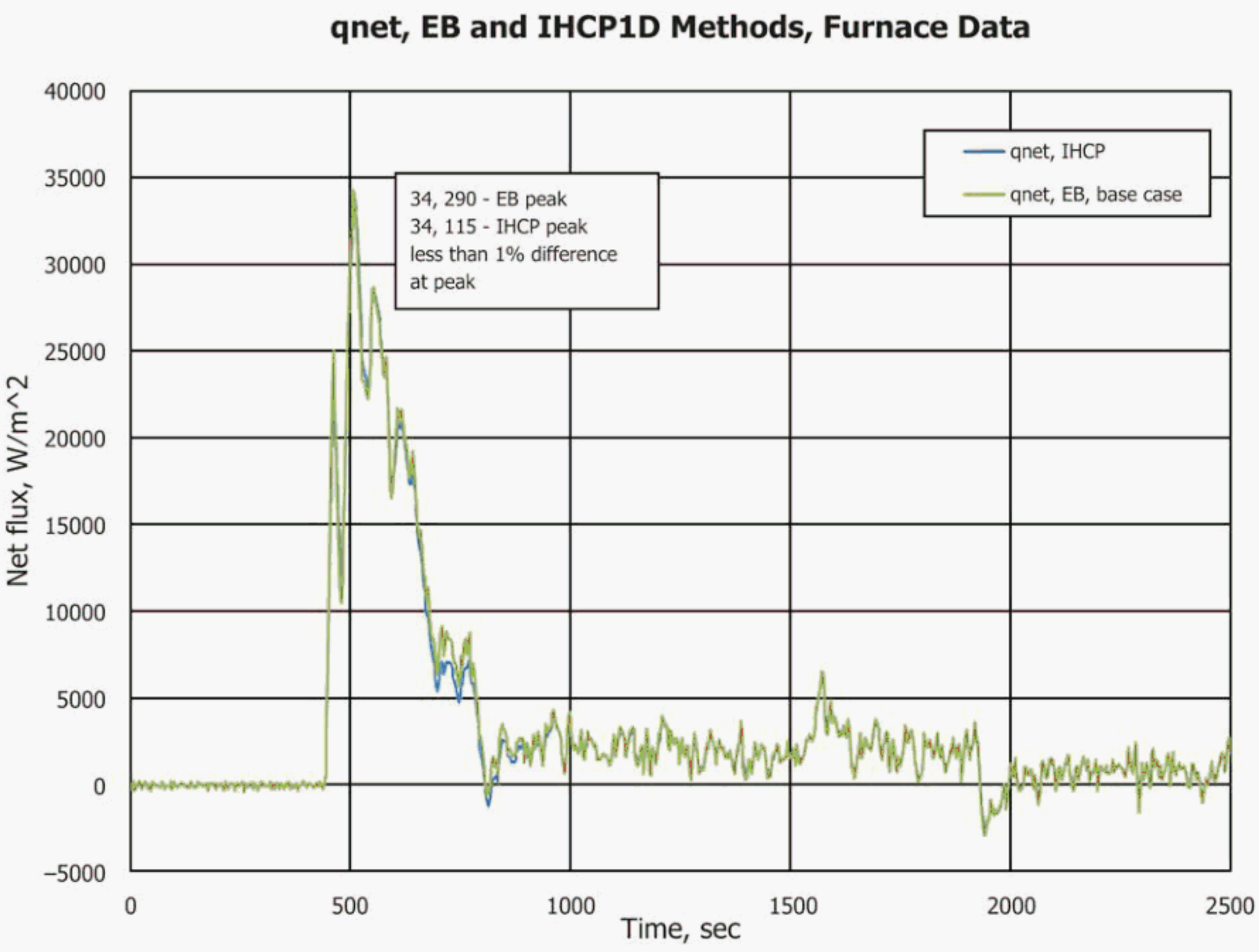

FIG. X5.2 Net Heat Flux from IHCP1D and Energy Storage Methods

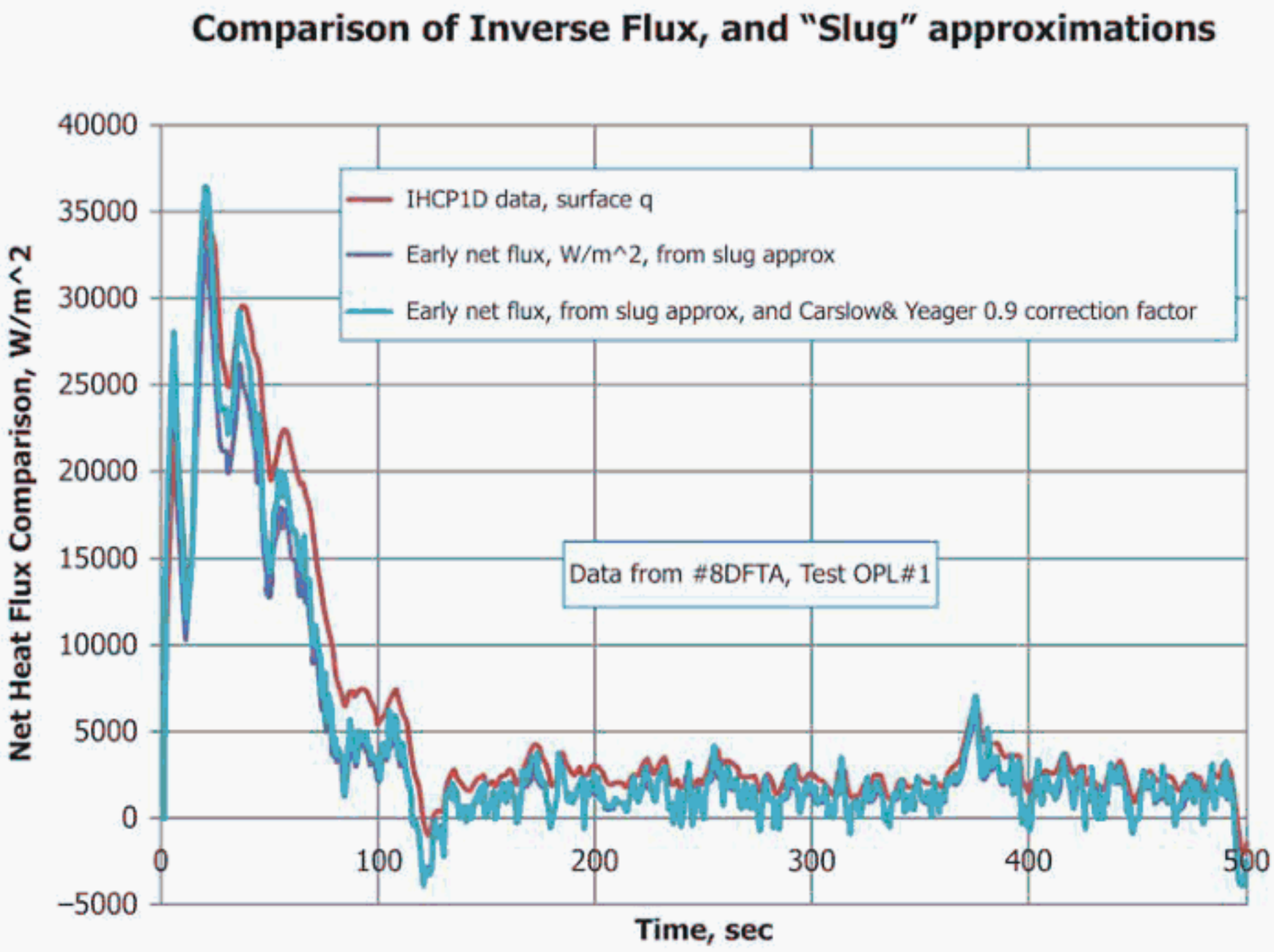

FIG. X5.3 Comparison of Net Heat Flux from Inverse HC and Early Time (Slug) Approximations

(Eq X4.1) show good qualitative agreement, but in some cases only fair quantitative agreement. The slug approximations are most often lower than the inverse calculations. The inverse calculations show lower fluctuations due to the "smoothing" nature of inverse calculations.

X5.1.5 Note that when using the slug approximations, it is important to use temperature dependent values for the specific heat (cp) rather than a single average value. For example, over the first 300 sec, the plate temperature rise is about 640 °C, and the specific heat increases by about 26 %.

X5.1.6 Fig. X5.4 shows a comparison of $T_{effective}$ (Eq X4.4, Appendix X4) and T_{DFT}. $T_{effective}$ and T_{DFT} are very different at early times, but very close after about 400 sec.

X5.1.7 Fig. X5.5 shows a comparison of the "Thermal Exposure" from Eq X4.2 (Appendix X4), and the very late time flux, which is the incident radiative flux, from Eq X4.5. The thermal exposure (based on $T_{effective}$) is more accurate at early times than is the "very late flux," as one might expect.

X5.1.8 Fig. X5.6 shows a comparison of the measured DFT temperature ("EXP T(1)"), which is located on the unexposed side of the plate, and two other temperatures calculated by

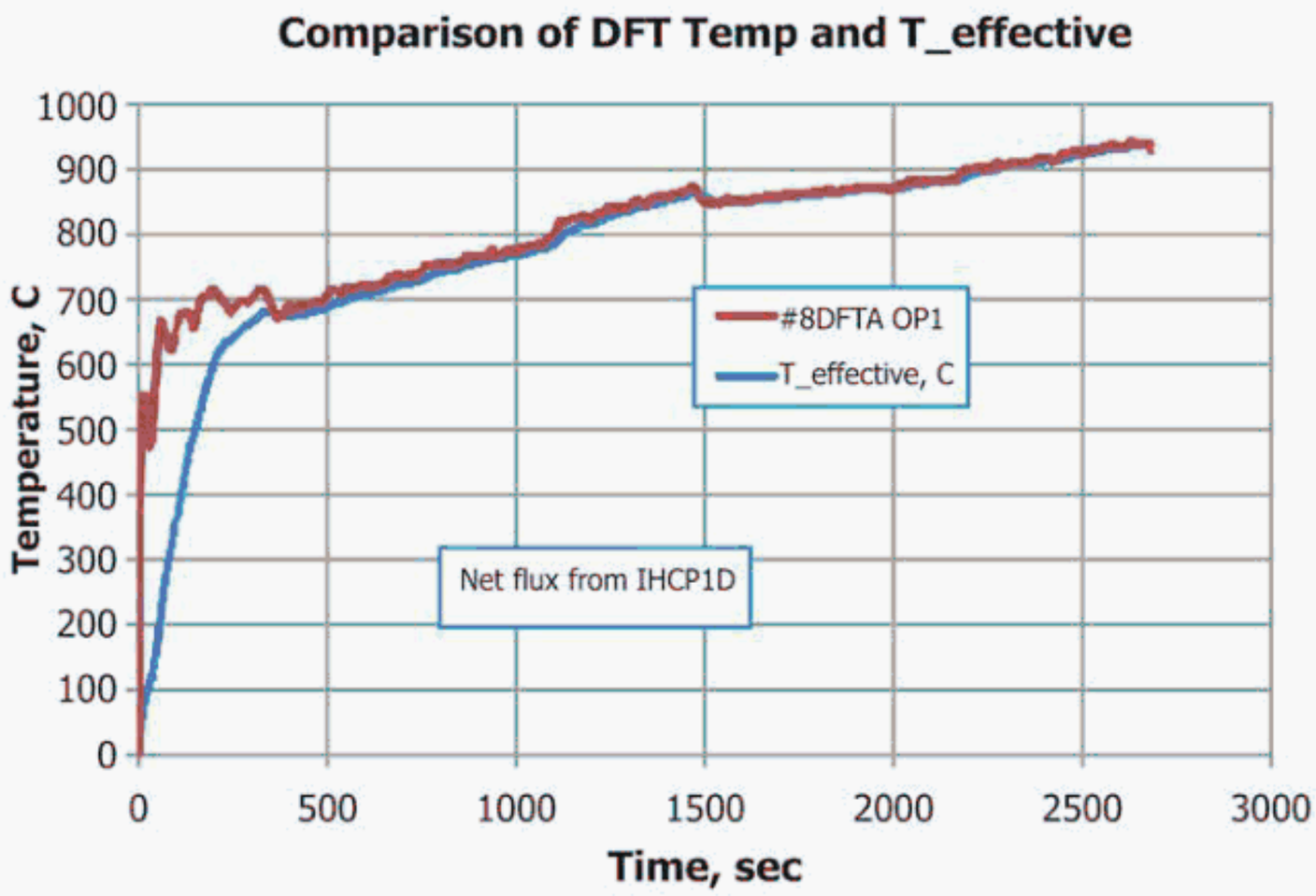

FIG. X5.4 Comparison of $T_{effective}$ and T_{DFT}

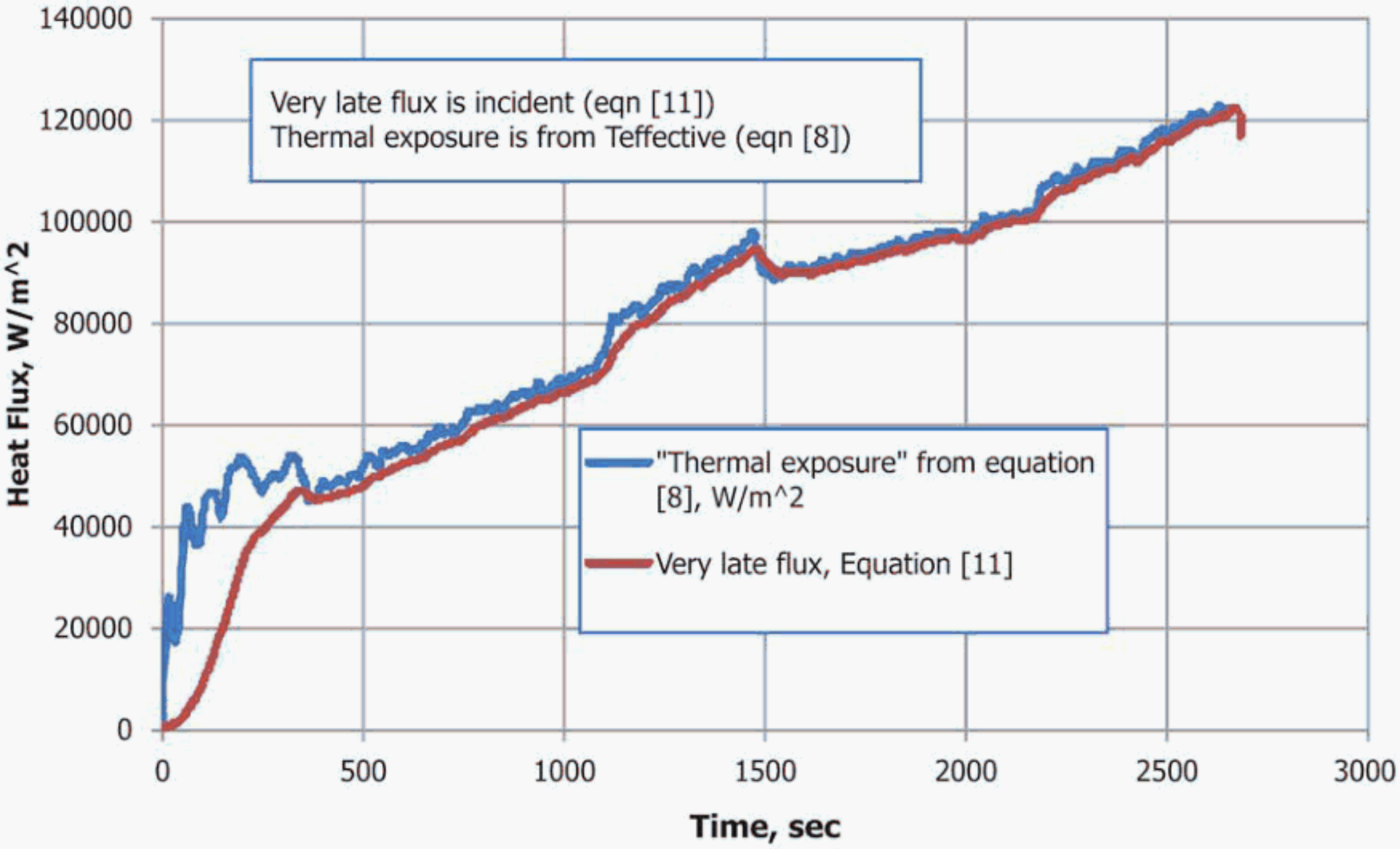

FIG. X5.5 Comparison of Thermal Exposure and Very Late (Incident) Flux

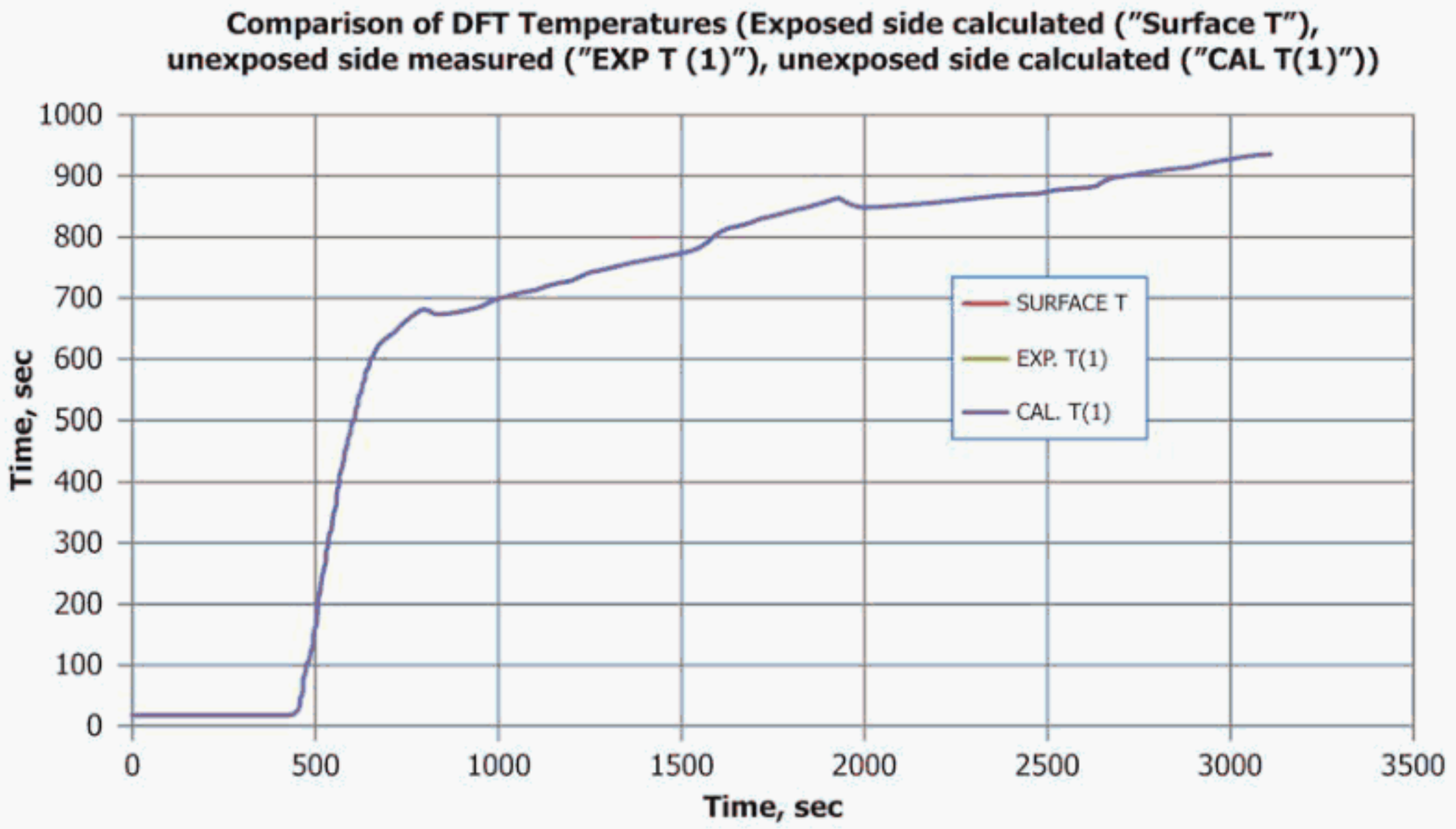

FIG. X5.6 Comparison Between DFT Temperatures
(Measured on Unexposed Side, Calculated on Unexposed Side, and Calculated, Exposed Side)

IHCP1D (or any other inverse codes like SODDIT) ("SURFACE T", and "CAL T(1)"). "SURFACE T" is the calculated exposed surface temperature of the plate, and "CAL T(1)" is the calculated temperature on the unexposed side (CAL T(1) should equal EXP T(1)). The three values are so close as to make them indistinguishable. Differences between the measured and calculated unexposed side temperatures were less than ±4 °C throughout the entire test. This suggests that, for furnace tests, the differences between the exposed and unexposed side temperatures are negligible. This was a key assumption made in Eq 7. Therefore, dT_{DFT}/dt in Eq 7 can be accurately estimated in furnace tests using the measure (unexposed side) temperature. This is important because TCs mounted on the exposed side of the DFT are generally less reliable compared with TCs mounted on the exposed side. Also, TCs on the exposed side typically suffer from a bias error

(the TC reads higher than the plate temperature), so the exposed side reading should be corrected for the bias error.

BIBLIOGRAPHY

(1) Keltner, N. R., and Wildin, M. W., "Transient Response of Circular Foil Heat-Flux Gauges to Radiative Fluxes," *Review of Scientific Instruments*, Vol 46, No. 9, Sept., 1975, pp. 1161–1166.

(2) Keltner, N. R., amd Wildin, M. W., "Transient Response of Circular Foil Heat Flux Gauges to Radiative Fluxes," *Rev. Sci. Instrumentation*, Vol 46, No. 9, September 1975.

(3) Borell, G. J., and Diller, T. E., "A Convection Calibration Method for Local Heat Flux Gauges," *ASME Journal of Heat Transfer, Transactions of the ASME*, Vol 109, February 1987, pp. 83–89.

(4) Gifford, A. R., Hubble, D. O., Pullins, C. A., Huxtable, S. T., and Diller T. E., (2010) "A Durable Heat Flux Sensor for Extreme Temperature and Heat Flux Environments," *AIAA Journal of Thermophysics and Heat Transfer*, 24, pp. 69–76.

(5) Gritzo, L. A., et al., "Thermal Measurements to Characterize Large Fires," Proceedings of the 41st International Instrumentation Symposium, Aurora, CO, May, 1995, pp. 337–346.

(6) Young, C. N., "Thermocouple Compensation," MS Thesis, University of Waterloo, Waterloo, Ontario, Canada, 1998.

(7) Sobolik, K. B., Keltner, N. R., and Beck, J. V., "Measurement Errors for Thermocouples Attached to Thin Plates: Application to Heat Flux Measurement Devices," *ASME HTD – Vol. 112, Heat Transfer Measurements, Analysis, and Flow Visualization*, Edited by R. K. Shah, 1989.

(8) Kuo, C. H., and Kulkarni, A. K., "Analysis of Heat Flux Measurement by Circular Foil Gauges in a Mixed Convection/ Radiation Environment," *ASME/JSME Thermal Engineering Proceedings*, Volume 5 – ASME 1991.

(9) Keltner, N. R., "Thermal Measurements in Fire Safety Testing – Are We Playing with Fire?" Special Symposium of Fire Calorimetry, NIST, Gaithersburg, MD, July, 1995, Fire Calorimetry Proceedings, Editors: Hirschler and Lyon, DOT/FAA/CT-95/46, FAA Tech Center, Atlantic City Int'l Airport, NJ.

(10) Gifford, A., Hoffie, A., Diller, T., and Huxtable, S., "Convection Calibration of Schmidt-Boelter Heat Flux Gauges in Stagnation and Shear Air Flow," *Journal of Heat Transfer*, 132, 2010 (031601-1 through 031601-9).

(11) Nakos, J. T., et al., "An Analysis of Flame Temperature Measurements Using Sheathed Thermocouples in JP-4 Pool Fires," Proceedings of the ASME / JSME Engineering Joint Conference, Editors: J. R. Lloyd and Y. Kurosaki, ASME Book No. I0309E, 1991, pp. 283–289.

(12) Burgess, M. H., "Heat Transfer Boundary Conditions in Pool Fires," IAEA-SM-286 / 75P, PATRAM'86.

(13) Fry, C. J., "Pool Fire Testing at AEE Winfrith," AEE Winfrith, Dorchester, UK, Proceedings of the 9th International Symposium on Packaging and Transportation of Radioactive Materials (PATRAM'89), Washington, D.C., June 1989.

(14) Burgess, M. H, and Fry, C. J., "Fire Testing for Package Approval," *Int'l. Journal of Radioactive Materials Transport (RAMTRANS)*, Vol 1, No. 1, 1990, pp. 7–16.

(15) Fry, C. J., "An Experimental Examination of the IAEA Fire Test Parameters," AEE Winfrith, Dorchester, UK, circa 1992.

(16) Keltner, N. R., "Directional Flame Thermometers: A Tool for Measuring Thermal Exposure in Furnaces and Improving Control," Proceedings of the Interflam 2007 Conference (CD version only), University of London, UK, Sept. 3–5, 2007.

(17) Keltner, N. R., et al., "Using Directional Flame Thermometers for Measuring Thermal Exposure," ASTM E5 Symposium on Advances in the State of the Art of Fire Testing, Miami Beach, FL, December, 2008. Published in the *Journal of ASTM International*, Vol 7, No. 2, 2010, Paper ID JAI102280.

(18) Janssens, M., "Comparison of Different Methods to Characterize the Thermal Environment in Fire Resistance Furnaces," ISO/TC92/SC2 Workshop on Heat Transfer Calculations and Measurements in Fire Safety Engineering, held Sept., 2007 at SP Swedish National Testing and Research Institute, Boras, Sweden.

(19) Wittasek, N. A. "Analysis and Comparison of Marine Fire Testing Regulations and Procedures," Master of Science Thesis, Worcester Polytechnic Institute, Worcester, MA, 1996.

(20) Beyler, C., et al., "Fire Resistance Testing for Performance-Based Fire Design of Buildings," The Fire Protection Research Foundation, Quincy, MA, June, 2008.

(21) Tieszen, S. R., "Prescriptive vs. Performance Based Cook-Off Fire Testing," Department of Defense Explosives Safety Seminar, Portland, OR, July 13–15 2010.

(22) Sultan, M., "Fire Resistance Furnace Temperature Measurements: Plate Thermometers vs Shielded Thermocouples," *Fire Technology*, Vol 42, No. 3, July 2006, pp. 253–267.

(23) Sultan, M., "Comparisons of Measured Temperature and Heat Flux in Fire Resistance Test Furnaces Controlled by either ISO Plate Thermometers or by ASTM Shielded Thermocouples or by Directional Flame Thermometers," ASTM E5 Symposium on Advances in the State of the Art of Fire Testing, Miami Beach, FL, December 2008.

(24) Pullins, C. A., and Diller, T. E., "In situ High Temperature Heat Flux Sensor Calibration," *International Journal of Heat and Mass Transfer*, 53, 2010, pp. 3429–3438.

(25) Trelewicz, J. R., Longtin, J. P., Hubble, D. O., and Greenlaw, R. J., "High-Temperature Calibration of Direct Write Heat Flux Sensors From 25C to 860C Using the In-Cavity Radiation Method," *IEEE Sensors J.*, Vol 15, 2015, pp. 358–364.

(26) Figueroa, V. G., and Nakos, J. T., Fire Science and Technology, Department 9132, Sandia National Laboratories, and J. E. Murphy, Worcester Polytechnic Institute, "Uncertainty Analysis of Heat Flux Measurements Estimated Using a One-Dimensional Inverse Heat Conduction Program," Sandia Report SAND2005-339, Albuquerque, NM, February, 2005.

(27) Figueroa, V. G., "Emittance of Inconel® 600, SS304, 17-4PH™ Stainless Steel, Aluminum 7075 and Mk 4 Aeroshell," Sandia National Laboratories memorandum to Distribution, May 10, 2005.

(28) Figueroa, V. G., "Mineral-Insulated, Metal Sheathed Thermocouple Bias Errors," Sandia National Laboratories memorandum to Distribution, April 18, 2005.

(29) Brundage, A., Kearney, S., Donaldson, B., Nicolette, V., and Gill, W., "A Joint Computational and Experimental Study to Evaluate Inconel-Sheathed Thermocouples Performance in Flames," Sandia National Laboratories report SAND2—5-3978, Printed August 2005.

(30) Reed, R. P., "Ya Can't Calibrate a Thermocouple Junction! Part 1 - Why Not?" *Measurements & Control*, September 1996, pp. 137–145.

(31) Reed, R. P., "Ya Can't Calibrate a Thermocouple Junction! Part 2 - So What?" *Measurements & Control*, October 1996, pp. 93–100.

(32) Beck, J. V., et al., *Inverse Heat Conduction: Ill-Posed Problems*, Wiley Interscience, 1985, ISBN0-471-08319-4, (this book is out of print – a PDF is available from the author).

(33) Beck, J. V., "User's Manual for IHCP1D – Program for Calculating Surface Heat Fluxes from Transient Temperatures in Solids," Beck Engineering Consultants Co., Okemos, MI, 1999.

(34) Blackwell, B. F., Douglass, R. W., and Wolf, H., "A User's Manual for the Sandia One-Dimensional Direct and Inverse Thermal (SODDIT) Code," Sandia National Laboratories report SAND85-2478, UC-32, Printed May 1987, and Reprinted December 1990.

(35) Beck, J. V., "Filter Solutions for the Nonlinear Inverse Heat Conduction Problem," *Inverse Problems in Science and Engineering*, 16, 2008, pp. 3–20.

(36) Blanchet, T. K., et al., "Sandia Heat Flux Gauge Thermal Response and Uncertainty Models," Sandia National Laboratories, SAND 2000-1111, May 2000.

(37) Nakos, J., and Engerer, J., "Data Reduction Tools and Uncertainty Analysis of Incident Heat Flux Measurement Tools from Directional Flame Thermometers Used in Hydrocarbon Pool and Furnace Fires," Sandia National Laboratories report SAND2018-10332, September 2018.

(38) Incropera, F. P., and DeWitt, D. P., *Fundamentals of Heat and Mass Transfer, Fifth Edition*, John Wiley & Sons, 2002, p. 281.

(39) Bryant, R., Womeldorf, C., Johnsson, E., and Ohlmiller, T., "Radiative Heat Flux Measurement Uncertainty," *Fire and Materials*, 27, 2003, pp. 209–222.

(40) Nakos, J. T., "Uncertainty Analysis of Steady State Incident Heat Flux Measurements in Hydrocarbon Fuel Fires," Sandia National Laboratories report SAND2005-7144, December 2005.

(41) Keltner, N. R., et al., "Fire Safety Test Furnace Characterization Unit," *Thermal Measurements: The Foundation of Fire Standards, ASTM STP 1427*, L. A. Gritzo and N. J. Alvares, Eds., ASTM International, West Conshohocken, PA, 2002, ISBN 0-8031-3451-7.

(42) Carslaw, H. S. and Jaeger, J. C., *Heat Conduction in Solids*, 2nd Edition, Oxford University Press, 1959 [Ch. 12.4. Eqn. 12].

(43) Keltner, N. R., et al., "Simulating Fuel Spill Fires Under the Wing of an Aircraft," Fire Safety Science – Proceedings of the Fourth International Symposium, Ottawa, Ontario, Canada, June, 1994, pp. 1017–1028, ISBN 1-886279-00-4.

(44) Noravian, H., et al., "Vulcan/Sinda Loosely Coupled Analysis Methodology for the NASA/JPL Rod Calorimeter," *JANNAF*, Boston, May 2008.

(45) Manzello, S. L., et al., Development of Rapidly Deployable Instrumentation Packages for Data Acquisition in Wildland-Urban Interface (WUI) Fires, *Fire Safety Journal*, 45, 2010, pp. 327–336.

(46) Heinonen, E. W., et al., "Inverted Deluge System (IDS) Development Tests, Volume I: Fire Suppression Tests," CEL-TR-92-71, New Mexico Engineering Research Institute, Albuquerque, NM, June 1992.

(47) Gill, W., and Nakos, J. T., "Temperature/Heat Flux Errors Caused by High Temperature Resistive Shunting Along Mineral-Insulated, Metal-Sheathed Thermocouples," Proceedings of the ASME Heat Transfer Division 1999, International Mechanical Engineering Congress and Exposition, Nashville, TN, November 14–18, 1999 (Vol 1), pp. 43–56.

(48) Keltner, N. R., Transient Thermal Analysis of Inconel Plate – Cerablanket Insulation, JPL Propellant Burn – Directional Flame Thermometers (DFTs), Ned Keltner, F.I.R.E.S, Inc., January 15, 2009.

(49) Wickstrom, U., "The Plate Thermometer – Practical Aspects," SP Swedish National Testing and Research Institute, SP Report 1997:28, Boras, Sweden, Sept., 1997.

(50) Babrauskas, V., and Williamson, R. B., "Temperature Measurements in Fire Test Furnaces," *Fire Technology*, Vol. 14, 1978, pp 226–238.

(51) Bainbridge, B. L., and Keltner, N. R., "Heat Transfer to Large Objects in Large Pool Fires," *Journal of Hazardous Materials*, Vol 20, December 1988, pp. 21–40.

(52) Blevins, L. G., and Pitts, W. M., "Modeling of Bare and Aspirated Thermocouples in Compartment Fires," *Fire Safety Journal*, 33, 1999, pp. 239–259.

(53) Cooke, G. M. E., "Can Harmonization of Fire Resistance Furnaces be Achieved by Plate Thermometer Control?" Fire Safety Science – Proceedings of the Fourth International Symposium, Ottawa, Ontario, Canada, June 1994.

(54) Gritzo, L. A., and Nicolette, V. F., Coupled Thermal Response of Objects and Participating Media in Fires and Large Combustion Systems, Numerical Heat Transfer, Part A, 28, 1995, pp. 531–545.

(55) Hubble, D. O. and Diller, T. E., "A Hybrid Method for Measuring Heat Flux," *ASME Journal of Heat Transfer*, 132, 2009, p. 8.

(56) Jakob, M., *Heat Transfer Volume II*, John Wiley & Sons, New York, 1957.

(57) Keltner, N. R. "What have We Learned about Uncertainty? Are We Still Playing with Fire?" ASTM E05 Symposium – Uncertainty and What to Do About It, 2011.

(58) Nakos, J. T., "The Systematic Error of a Mineral-Insulated, Metal Sheathed (MIMS) Thermocouple Attached to a Heated Flat Surface," *Thermal Measurements: The Foundation of Fire Standards, ASTM STP 1427*, L. A. Gritzo and N. J. Alvares, Eds., American Society for Testing and Materials, West Conshohocken, PA, 2002.

(59) Preist, D., Private Communication, Intertek – Omega Point Laboratories, 2004.

(60) Raphael-Mabel, S., Huxtable, S., Gifford, A., and Diller, T., "Design and Calibration of a Novel High Temperature Heat Flux gauge," HT2005-72761, Proceedings of HT2005, 2005 ASME Summer Heat Transfer Conference, July 17–22, San Francisco, CA.

(61) Robertson, A. F., and Ohlemiller, T. J., "Low Heat Flux Measurements: Some Precautions," *Fire Safety Journal*, 25, 1995, pp. 109–124.

(62) Wickstrom, U., "Adiabatic Surface Temperature for Calculating Heat Transfer to Fire Exposed Structures," Proceedings of the Interflam 2007 Conference, University of London, UK, Sept. 3–5, 2007.